

HELSINKI UNIVERSITY OF TECHNOLOGY
Department of Electrical and Communications Engineering
Laboratory of Acoustics and Audio Signal Processing

Miikka Tikander

Model-based curvefitting for in-situ impedance measurements

Master's Thesis submitted in partial fulfillment of the requirements for the degree of Master of Science in Technology.

Espoo, March 8, 2003

Supervisor: Professor Matti Karjalainen

Author:	Miikka Tikander	
Name of the thesis:	Model-based curvefitting for in-situ surface impedance measurements	
Date:	Mar 8, 2003	Number of pages: 68
Department:	Electrical and Communications Engineering	
Professorship:	S-89	
Supervisor:	Prof. Matti Karjalainen	
<p>For an acoustics designer it is important to be able to measure the acoustical properties of materials and surface structures in the actual place where the material is placed. In this work various <i>in-situ</i> methods for measuring the acoustical surface impedance are studied.</p> <p>In-situ measurement techniques can be roughly divided into two main categories: free field methods and windowing methods. When measuring in-situ, the effect of the apparent error sources, e.g., reflection from surrounding surfaces and from the measurement device itself, must be carefully taken into account. As a new idea, using a hard surface measurement as reference in subtraction method is introduced to increase the robustness of the measurement technique.</p> <p>As another new idea, model-based curvefitting is introduced. When there is knowledge about the material or the surface structure, an acoustical model of the surface can be formed. This model can be fitted to the measured data and if the model is valid the robustness and reliability of the measurement can be increased. Delany and Bazley have formed empirical models for characteristic impedance and propagation constant in porous materials. The applicability of these models for model-based curvefitting is tested. Also, an abstract model for reflection at the surface of a homogeneous wool-like material on a hard surface is created and tested. In general, in-situ methods work well with fairly absorptive material. At low frequencies and when measuring materials with little absorption all in-situ methods are found troublesome.</p> <p>This work has been carried out as a part of the TEKES-project VÄRE/TAKU, where the objective of one of the subproject was to study the acoustical behavior of materials and acoustical measurement techniques. All the measurements performed in this work are compared with impedance tube and reverberation room measurements.</p>		
<p>Keywords: in-situ, surface impedance, modeling, acoustics</p>		

TEKNILLINEN KORKEAKOULU DIPLOMITYÖN TIIVISTELMÄ

Tekijä:	Miikka Tikander	
Työn nimi:	Mallipohjainen käyränsovitus in-situ pintaimpedanssimittauksiin	
Päivämäärä:	8.3.2003	Sivuja: 68
Osasto:	Sähkö- ja tietoliikennetekniikka	
Professori:	S-89	
Työn valvoja:	Prof. Matti Karjalainen	
<p>Akustisen suunnittelun kannalta on tärkeää, että akustinen pintaimpedanssi pystytään luotettavasti mittaamaan paikan päällä (<i>in-situ</i>), missä tutkittava materiaali tai pintarakenne sijaitsee. Tässä työssä esitellään erilaisia in-situ-menetelmiä akustisen pintaimpedanssin mittaamiseen.</p> <p>In-situ-mittaustekniikat voidaan käytännössä jakaa kahteen pääkategoriaan: vapaakenttä- ja ikkunointimenetelmään. Lisäksi yhtenä erilaisena metodina voidaan erotella ns. vähennystekniikkaa. In-situ-mittauksissa on erityisen tärkeä kiinnittää huomiota erilaisiin häiriölähteisiin, kuten ympäröivät pinnat ja itse mittalaitteesta aiheutuvat haitalliset heijastukset. Uutena ideana esitellään kovan pinnan käyttö refe-renssinä vähennystekniikkaan perustuvassa mittauksessa. Tällä menetelmällä voidaan mittalaitteesta aiheutuvien haitallisten heijastusten vaikutusta pienentää.</p> <p>Toisena uutena asiana esitetään mallipohjainen käyränsovitus in-situ-mittauksissa. Kun mitattavasta materiaalista tai rakenteesta on tietoa, voidaan pinnasta tehdä akustinen malli. Näin muodostettu malli voidaan sovittaa pinnan mitattuun vasteeseen ja mikäli malli on pätevä, voidaan näin parantaa mittausten luotettavuutta. Delany ja Bazley ovat esittäneet empiiriset mallit huokoisten materiaalien karakteristiselle impedanssille ja etenemiskertoimelle. Näiden mallien soveltuvuutta mallipohjaiseen käyränsovitukseen testataan. Lisäksi esitellään ja testataan abstrakti malli heijastukselle tapauksessa, jossa homogeeninen villamainen absorbentti on kovalla pinnalla. In-situ menetelmät toimivat melko hyvin mitattaessa materiaaleja, joissa on suhteellisen paljon abroptiota. Sen sijaan pienillä taajuuksilla ja mitattaessa heikosti absorboivia materiaaleja menetelmät toimivat heikosti.</p> <p>Tämä työ on tehty osana TEKES-projektia VÄRE/TAKU. Projektin yhden osion tavoitteena oli tutkia ja kehittää erilaisia materiaalien akustisten parametrien mittaustekniikoita. Projektin toisessa osassa suoritettiin suuri määrä mittauksia impedanssiputki- ja kaiuntahuonemenetelmillä eri materiaaleilla. Näitä mittauksia on käytetty vertailukohteena tässä työssä mitattuihin tuloksiin.</p>		
Avainsanat: in-situ, akustinen pintaimpedanssi, mallintaminen, akustiikka		

Preface

This work has been carried out in the Laboratory of Acoustics and Audio Signal Processing, Helsinki University of Technology, during years 2001-2002.

First, I would like to deeply thank Professor Matti Karjalainen for supervising this work and for giving me an opportunity to be part of the wonderful staff of the acoustics laboratory. His guidance and experience in all areas of acoustics have a big contribution to the outcome of this work.

I would like to thank the acoustics lab staff for making every working day a new adventure. Everybody has always been very helpful whenever there has been a need of an advice or any other matter. I couldn't imagine a better working environment. Especially, I would like to thank Lea Söderman for helping with all the running errands and Toomas Altosaar for many enjoyable discussions in all areas of life and work.

This work has been done as part of the VÄRE/TAKU-project. I would like to thank all people in the project who have helped me in my work, especially Timo Rankonen's material measurements have been very helpful along the project.

I would also like to thank my parents for guiding me on this road of studying and for supporting me in various ways.

And finally, I would like show my deepest gratitude to my loving wife Tiina for endless support and for making my life outside work another adventure.

Otaniemi, December 31, 2002

Miikka Tikander

Contents

1	Introduction	7
2	Theory	9
2.1	Sound wave propagation	9
2.1.1	Plane waves	9
2.1.2	Spherical waves	13
2.2	Acoustic impedance	13
2.3	Reflection coefficient	14
2.3.1	Spherical wave reflection	16
2.4	Reflection at oblique incidence	16
2.5	Local reaction	17
2.6	Absorption	18
2.7	Losses in the material	18
2.8	Impulse response measurement	20
2.9	Laboratory measurements of acoustic materials	21
2.9.1	Impedance tube method	21
2.9.2	Reverberation room method	22
3	In-situ measurements	24
3.1	Introduction	24
3.2	Free-field method	27
3.2.1	One microphone	27
3.2.2	Two microphones	29
3.3	Windowing method	30
3.4	Subtraction method	31
3.4.1	Using hard surface as reference	33
4	Error sources in measurements	35
4.1	The plane wave assumption	35
4.2	Parasitic reflections from the source	37

4.3	Source directivity	39
5	Model-based curve fitting	42
5.1	Introduction	42
5.2	Acoustic wave propagation models	43
5.2.1	Delaney-Bazley	43
5.2.2	Mechel	43
5.2.3	Allard-Champoux	44
5.3	Abstract models	45
5.4	Curve fitting	47
5.4.1	Fitting the propagation models	48
5.4.2	Fitting the abstract system models	49
6	Results	50
6.1	Hard surface reference for subtraction method	51
6.2	Model-based curve fitting	51
7	Discussion	54
8	Conclusions	55
A	Appendix	56
A.1	Materials	56
A.2	System setup	57
A.2.1	Microphone	57
A.2.2	Loudspeaker	57
A.2.3	Software	57
A.2.4	Amplifiers	58
B	Appendix	59
B.1	Measurement data	59
B.1.1	Using hard surface as reference	59
B.1.2	Model-based curvefitting	61

Abbreviations

p_0	Static air pressure
A	Area
p	Air pressure
m	Mass
a	Acceleration
F	Force
S/N	Signal to noise ratio
THD	Total harmonic distortion
f	Frequency
α	Absorption coefficient
ζ	Specific impedance
R	Reflection coefficient
λ	Wave length
\mathbf{r}	Receiver distance from the source
ρ_0	Density of air at steady state
ρ	Density of air
ξ	Displacement of an volume element
κ	Bulk modulus of elasticity
u	Particle velocity
u_n	Normal component of the particle velocity
Z_0	Characteristic impedance of air
Z_n	Surface impedance
c	Phase velocity, speed of sound
ω	Angular velocity
λ	Wave length
k	Wave number
Φ	Phase angle of the reflection angle
s	Standing wave ratio
r	Reflection coefficient
Z_a	Acoustic impedance
γ	Ratio of specific heats

1 Introduction

Acoustical properties of materials have been measured for a very long time. The conventional methods, Kundt's impedance tube and the reverberation room, have been studied and used as references for decades. Though the methods, just mentioned, don't bring much comfort in place where an engineer is building a listening room, for example. Impedance tube measurements require carefully cut samples of the material which might sometimes be quite impossible when working in the field. The reverberation room measurement, on the other hand, needs to be done in a special reverberation room. This already makes it quite impractical solution for an in-field method.

Wall and other surface structures are rarely something used in the reference books. That is where in-situ measurement is a welcome tool for an engineer. If there were a reliable way to measure the acoustical properties of a surface *in-situ*, it would make acoustical designing much faster and reliable - and more cost worthy, of course.

This work has been done as a part of the TEKES-project VÄRE/TAKU, where the objective of one of the subproject was to study the acoustical behavior of materials and acoustical measurement techniques. The main goal of the in-situ measurement part was to study and develop in-situ surface impedance measurement techniques.

In-situ measurement techniques have been studied for quite a long time and various measurement techniques have been proposed. As the in-situ measurements are done in the actual place where the material is placed, the measurements face many challenges not present in laboratory conditions. Especially the surrounding surfaces interfere the measurements. Quite often the measurement device needs to be taken close to the surface under study and this way the measurement device distracts the measurement as well. Many of the measurement techniques rely on some sort of an ideal reference measurement, e.g., in front of a hard surface. Performing such a reference measurement in-situ may turn out to be problematic in some cases. On the other hand, when these restrictions are acknowledged the in-situ measurements techniques can be used as a very useful acoustic field measurement tool.

In this work two new ideas are introduced to improve the robustness and usability of the in-situ measurement techniques: using hard surface measurement as a reference in subtraction measurement technique and the model-based curve fitting for in-situ surface impedance measurements. When the measurement device is taken close to the

surface the parasitic reflections from the device itself degrade the measurement data, and at worst case ruin the data completely. By using the hard surface measurement as a reference in the subtraction method the interfering effect of the measuring device can be decreased considerably. Although the measurements seem to give good results with this method the topic should still be studied further in order to understand the phenomena more thoroughly.

Quite often there is information about the surface structure under study. When the surface structure is known, an acoustic model could be formed and this model can be fitted to the measurement data. This way the measurement results could be checked whether they obey the assumed behavior of the surface structure. Especially at low frequencies the reliability of the measurement can be increased. In order for this method to work, good models with few parameters are needed. There are lots of acoustical models for different kinds of materials but most of them have too many free parameters for practical curvefitting. Ideally the model would have only one or two free parameters. In this work the empirical models for characteristic impedance and propagation constant of homogeneous and fibrous absorbents, first introduced by Delany and Bazley, are used and tested how they work in curvefitting.

The model doesn't need to have a direct physical background. Basically any model that behaves the same way as the surface structure could be used. As an example, an abstract model for reflection at the surface of a homogeneous, wool-like absorbent on a hard wall was created and tested. In general, abstract models are suitable only for simple cases.

The in-situ techniques seem to work fairly good with absorptive materials and at the frequency range from few hundred Hz to few kHz. Especially at low frequencies, where the wavelengths are much longer than the measurement distance and often there is also less absorption, the in-situ techniques are very sensitive to all kinds of interference.

This work has been structured as follows. In the second chapter the necessary theory for this topic is introduced. Also the traditional laboratory measurement methods, Kundt's impedance tube and the reverberation room method, are explained, as these are often used as reference methods. The third chapter first goes through the literature concerning the in-situ measurement techniques and then the main methods are introduced more thoroughly. The error source in in-situ measurements are gone through in chapter four. The model-based curvefitting is introduced in chapter five. The curvefitting is first applied by using empirical models for acoustical wave propagation in materials and then an abstract model for reflection at the surface of a wool-like absorbent is introduced and tested. Chapter six shows the result obtained by using a hard surface as reference in the subtraction method and by using the model-based curvefitting.

2 Theory

2.1 Sound wave propagation

In a steady state, with no sound sources, all the molecules of air are in a continuous movement. Due to a temperature agitation the molecules are moving to all directions in a very indeterministic manner. Molecules are hitting each other and changing the direction of movement all the time. However, in average the net movement of molecules is zero - meaning that no energy is moving in the air. This constant agitation causes a *static pressure*, p_0 , of about 10^5 Pa that is always around us. [22]

If there is some kind of a sound source present e.g. a loudspeaker, and it is feed with an impulse, the cone moves out wards and hits the molecules close to the surface causing them to move to the same direction. This also compresses the air in that place resulting in a higher pressure. Just like when a stone is dropped in a pond, the pulse starts spreading away from the source. Though in the case of an air wave the spreading happens in all three dimensions like shown in Figure 1b.

Let's first consider the propagation of *plane waves* of sound. In this case the whole wave is moving to the same direction perpendicular to the crest of the wave (see Figure 1a) - like a big wall moving. Waves traveling along the inside of a tube with a uniform cross section are often very close to plane waves. Also when the waves are studied a long distance away from the source, they are also very close to plane waves.

2.1.1 Plane waves

Like stated above, p_0 is the static air pressure and ρ_0 the density of the air. For static case, these are constant throughout the space. Though air consists of small particles, molecules, it can be considered to consist of small volume elements. As shown in Figure 2, the volume of the element is $A dx$. Now, if the volume element is set to motion the pressures on either side of the element are different. The pressure difference and the initial disturbing force result the section A to displace an amount of ξ and the section A' an amount of ξ' . The volume of the disturbed element is

$$A [dx + (\xi - \xi')] = A(dx + d\xi). \quad (1)$$

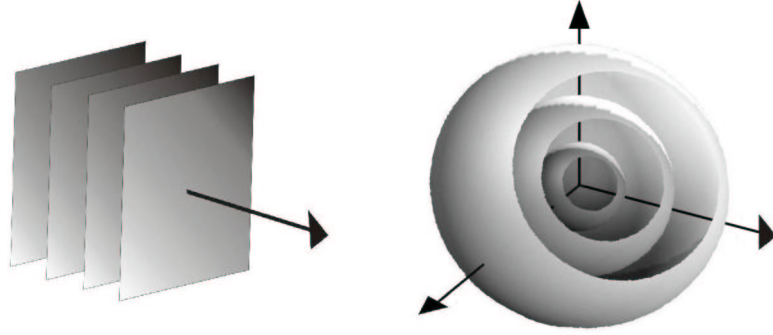


Figure 1: Propagation of a) plane waves and b) spherical waves.

Because of change in the volume there also has to be a change in density as well. The mass of the undisturbed element is $\rho_0 A dx$. If ρ is the density of the disturbed element, its mass is $\rho A(dx + d\xi)$. The conservation of matter requires these both masses to be equal,

$$\rho A(dx + d\xi) = \rho_0 A dx \quad (2)$$

This can be rewritten in the form

$$\rho = \frac{\rho_0}{1 + \partial\xi/\partial x}. \quad (3)$$

If $\partial\xi/\partial x$ is small, which generally is the case, we can use an approximation $(1 + k)^n \approx (1 + nk)$ yielding $\rho = \rho_0(1 - \partial\xi/\partial x)$ or

$$\rho - \rho_0 = -\rho_0 \left(\frac{\partial\xi}{\partial x} \right). \quad (4)$$

The pressure is related to the gas density ρ by an equation of state $p = f(\rho)$. Now, using the Taylor series, this function may be written as

$$p = p_0 + (\rho - \rho_0) \left(\frac{dp}{d\rho} \right)_{\rho=\rho_0} + \frac{1}{2} \rho - \rho_0^2 \left(\frac{d^2p}{d\rho^2} \right)_{\rho=\rho_0} + \dots \quad (5)$$

As the changes are assumed small, only the two first terms are kept. Now the relation can be written as

$$p = p_0 + (\rho - \rho_0) \left(\frac{dp}{d\rho} \right)_{\rho=\rho_0}. \quad (6)$$

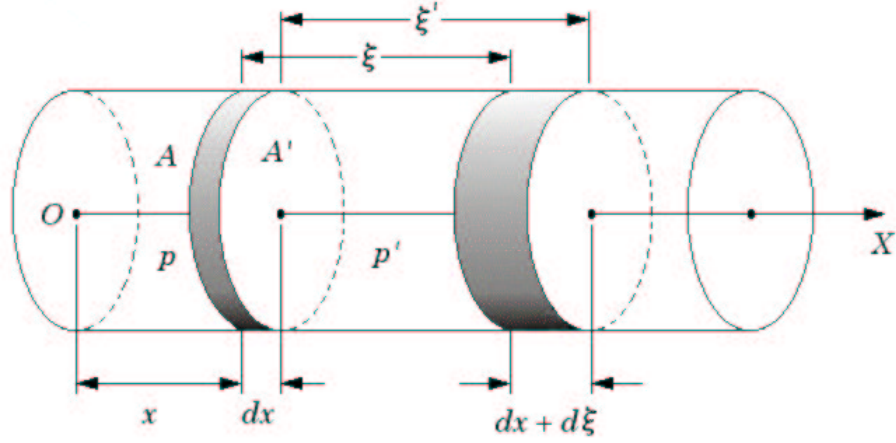


Figure 2: Compressional plane wave in a column.

By using the *bulk modulus of elasticity* κ the above equation (6) may be written as

$$p = p_0 + \kappa \left(\frac{\rho - \rho_0}{\rho_0} \right), \quad (7)$$

where κ is defined by the quantity

$$\kappa = \rho_0 \left(\frac{dp}{d\rho} \right)_{\rho=\rho_0}. \quad (8)$$

Now the equation (4) can be used to eliminate $(\rho - \rho_0)/\rho_0$ yielding

$$p = p_0 - \kappa \frac{\partial \xi}{\partial x}. \quad (9)$$

This expression relates the pressure at each point in the column to the amount of displacement from the equilibrium point.

The pressure difference on each side of the volume element causes a net force to the element. The pressure, p , on the left side causes a total force pA pushing to the right and the pressure p' on the right side causes a total force $p'A$ pushing to the left. The net force of the pressures is $(p - p')A$. Since $dp = p' - p$, the net force can be written as $-Adp$. The mass of the volume element is $\rho_0 Adx$ and its acceleration is marked as $a = \partial^2 \xi / \partial t^2$. Now the equation of motion ($F = ma$) can be written in the form

$$-Adp = (\rho_0 Adx) \frac{\partial^2 \xi}{\partial t^2} \quad (10)$$

or equivalently

$$\frac{\partial p}{\partial x} = -\rho_0 \frac{\partial^2 \xi}{\partial t^2}. \quad (11)$$

By taking the derivative of Equation (9) with respect to x and noting that p_0 is constant this yields

$$\frac{\partial p}{\partial x} = -\kappa \frac{\partial^2 \xi}{\partial x^2}. \quad (12)$$

Comparing Equation (12) with Equation (11) yields the *displacement* wave equation

$$\frac{\partial^2 \xi}{\partial t^2} = \frac{\kappa}{\rho_0} \frac{\partial^2 \xi}{\partial x^2} \quad (13)$$

On the other hand taking the second derivative of pressure in equation (9) with respect to time yields

$$\frac{\partial^2 p}{\partial t^2} = -\kappa \frac{\partial}{\partial x} \left(\frac{\partial^2 \xi}{\partial t^2} \right). \quad (14)$$

Now combining this with the Equation (11) yields the *pressure* wave equation

$$\frac{\partial^2 p}{\partial t^2} = \frac{\kappa}{\rho_0} \frac{\partial^2 p}{\partial x^2}. \quad (15)$$

As shown, the displacement and the pressure behave the same way obeying the wave equation. The wave propagates at the phase velocity c

$$c = \sqrt{\frac{\kappa}{\rho_0}}. \quad (16)$$

It is important to notice the difference between the phase velocity and the particle velocity. The phase velocity, c , expresses the velocity of a certain phase, e.g., a pressure maximum. This is what is generally called the speed of sound. The particle velocity, $u = \partial \xi / \partial t$, expresses the velocity of the displacement which vibrates around a certain point in the medium. The particle velocity is related to the pressure by the *characteristic impedance*, $Z_c = \rho_0 c$ of the medium.

$$u = \frac{p}{\rho_0 c} \quad (17)$$

A general solution for the wave equations is $\xi(x, t) = f(x \mp ct)$, which describes two waves traveling in opposite directions. Especially for harmonic case the solution can be written

$$\xi(x, t) = \xi_0 e^{-jk(x \mp ct)}, \quad (18)$$

where

$$k = \frac{2\pi f}{c} = \frac{2\pi}{\lambda} = \frac{\omega}{c} \quad (19)$$

is the *wave number* and λ is the *wavelength*.

Wave motion in air (and in other gasses) can be assumed to be an *adiabatic* process. This means that no energy is changed due to the heat flow. The wave motion causes pressure differences in the air and pressure relates to the temperature. Whenever there is a heat gradient the energy starts flowing away from the pressure maximum. This process is fairly slow and so if the pressure changes fast enough the heat doesn't have time to start flowing. Under adiabatic conditions $p = C\rho^\gamma$ where γ is the *ratio of specific heats* of the medium. For air under adiabatic conditions it has a value of 1.40. Now $dp/d\rho = \gamma C\rho^{\gamma-1}$ and combining this with the equation (8) yields $\kappa = \rho_0(dp/d\rho)_{\rho=\rho_0} = \gamma C\rho_0^\gamma$. This can be substituted in Equation (16) and the speed of sound¹ can be easily calculated as

$$c = \sqrt{\frac{\gamma p}{\rho}} \quad (20)$$

2.1.2 Spherical waves

Even though plane waves are a good and practical approximation in many situations, it is essential to acknowledge the spherical nature of waves. Figure 1 illustrates the wave propagation in both cases. If acoustic energy is assumed to be spread uniformly on each plane or sphere, it can be easily understood from the Figure 1 that the intensity stays constant in the plane wave, whereas in the spherical case it decreases with the distance from the source ($\sim 1/r^2$). [21, 4]

2.2 Acoustic impedance

In acoustics the impedance always relates the pressure to some velocity related quantity. The *acoustic impedance* Z_a is defined as the ratio of sound pressure p to volume

¹At 15⁰C the air pressure is 101.3 kPa and density is 1.229 kg/m³ yielding for the speed $c = 339.70 \approx 340$ m/s.

velocity q :

$$Z_a(f) = \frac{p}{q}. \quad (21)$$

The volume velocity q is the amount of air that flows through a specified area A , e.g., in the case of tube A would be the cross-sectional area of the tube. When u is the particle velocity of the medium the volume velocity can be written as $q = Au$. Acoustic impedance is analogous to electrical impedance, which is the ratio of voltage to electrical current.

The *characteristic impedance* is defined as the ratio of the pressure p and the normal component of the particle velocity u_n .

$$Z_c(f) = \frac{p}{u_n}. \quad (22)$$

For lossless materials the characteristic impedance can be written as $Z_c = \rho c$. For short distances air can fairly accurately be approximated to be lossless and the characteristic impedance of air can be written as $Z_0 = \rho_0 c$, where ρ_0 is the density of air and c is the speed of sound in air.

Quite often the characteristic impedance of a material is normalized to the characteristic impedance of air Z_0 . The ratio ζ between the characteristic impedance of the material and the characteristic impedance of air is called the *specific impedance*:

$$\zeta(f) = \frac{Z_n(f)}{\rho_0 c}. \quad (23)$$

Later in this work a term *surface impedance* Z_n will be used and it means the characteristic impedance at the surface of the material under study. [27, 22]

2.3 Reflection coefficient

Reflection coefficient $R(f)$ defines the ratio of the incident pressure p_i and the pressure p_r reflected from the surface

$$R(f) = \frac{p_r(f)}{p_i(f)}. \quad (24)$$

When both the incident and the reflected pressure waves are known the reflection coefficient and the impedance can be calculated. For the sake of simplicity the waves are assumed plane and air is assumed lossless. If the amplitude of the pressure wave is equal to one, the incident wave in Figure 3 is written as

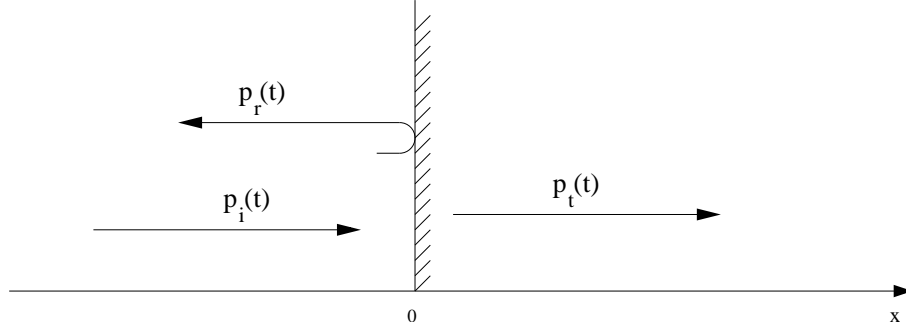


Figure 3: Reflection of a pressure wave on a boundary.

$$p_i(x) = e^{jkx}. \quad (25)$$

When the wave reaches the material, part of it goes through the surface and a part is reflected back. The reflected wave is

$$p_r(x) = Re^{-jkx}, \quad (26)$$

where R is the reflection coefficient. The corresponding particle velocities can be derived by using the characteristic impedance of air $Z_0 = \rho_0 c$ [Ns/m^3]:

$$u_i(x) = \frac{p_i(x)}{Z_0} \quad \text{and} \quad u_r(x) = -\frac{p_r(x)}{Z_0}. \quad (27)$$

The impedance seen by the total pressure field $p = p_i + p_r$ is

$$Z(x) = \frac{p_i(x) + p_r(x)}{u_i(x) + u_r(x)} = Z_0 \frac{p_i(x) + p_r(x)}{p_i(x) - p_r(x)}. \quad (28)$$

By substituting $p_i(t)$ and $p_r(t)$, the impedance $Z(x)$ can be written as

$$Z(x) = Z_0 \frac{e^{jkx} + Re^{-jkx}}{e^{jkx} - Re^{-jkx}}. \quad (29)$$

Now the impedance is a function of place and the properties of the surface. By setting $x = 0$ the impedance at the boundary can be solved

$$Z(0) = Z_0 \frac{1 + R(0)}{1 - R(0)}. \quad (30)$$

Also, if the impedance is known the reflection coefficient can easily be solved from the previous equation

$$R(0) = \frac{\zeta(0) - 1}{\zeta(0) + 1}, \quad (31)$$

where $\zeta(0) = Z(0)/\rho c$ is the specific impedance of the surface.

2.3.1 Spherical wave reflection

The plane wave assumption is applicable when the sound field is measured far ($r \gg \lambda$) away from the source. In the near field, which often is the case when measuring at low frequencies, the spherical nature of the wave has to be taken into account.

In 1946 Rudnick [28] studied the propagation of a spherical wave along a boundary. The work followed the solutions presented with the electromagnetic waves. The pressure field close to a surface can be written with a so-called Weyl-van der Pol equation:

$$p = \frac{e^{jk_1 r_1}}{r_1} + \frac{e^{jk_1 r_2}}{r_2} [(1 - R)F + R], \quad (32)$$

where R is the plane wave reflection coefficient and F is a function of angle, source distance, and material parameters of bounding surface. Practically this function accounts for the sphericity of the wave. With the distances much longer than the wave length ($r \gg \lambda$) or small angles or with highly reflecting surfaces the term F approaches 0. Thus the equation approaches

$$p \approx \frac{e^{jk_1 r_1}}{r_1} + R \frac{e^{jk_1 r_2}}{r_2}. \quad (33)$$

This is fairly often used approximation with the in-situ measurement techniques. According to Klein and Cops [15] the approximation is valid for angles of incidence up to 60° . The validity of the plane wave assumption will further studied in chapter 4.1.

2.4 Reflection at oblique incidence

Let's consider a case where a plane wave approaches the surface at an angle of θ_1 . As shown in Figure 4, a part of the wave reflects back at an angle of θ_3 and another part of the wave will penetrate in the material and diffract to an angle of θ_2 . According to Snell's law the incident and the diffracted angles are

$$\sin(\theta_2) = \frac{k_1}{k_2} \sin(\theta_1), \quad (34)$$

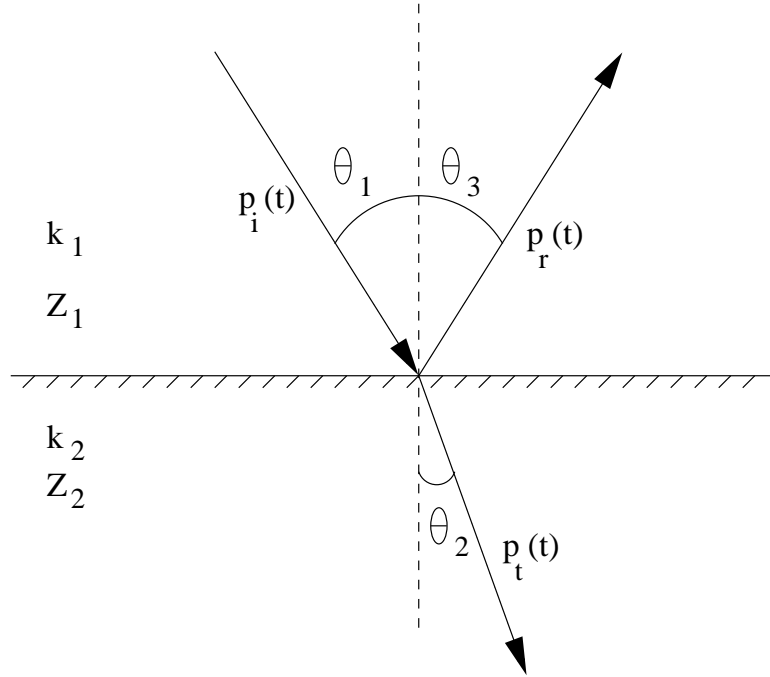


Figure 4: Transmission of a pressure wave on surface with extended reaction

where $k_i = \omega/c_i$. The reflection coefficient R is written as [22, 31]

$$R(\theta) = \frac{Z_2 \cos \theta_1 - Z_1 \cos \theta_2}{Z_2 \cos \theta_1 + Z_1 \cos \theta_2}. \quad (35)$$

2.5 Local reaction

In locally reactive materials the pressure field in the material is always normal to the surface [22]. Figure (5) shows how the wave passes a locally reacting boundary. Now $\cos \theta_2 = 1$ and equation (35) simplifies to

$$R(\theta) = \frac{z_2 \cos(\theta_1) - 1}{z_2 \cos(\theta_1) + 1}, \quad (36)$$

where $z_2 = Z_2/\rho c$. A surface constructed of thin tubes running through the material could be an example of a locally reacting surface.

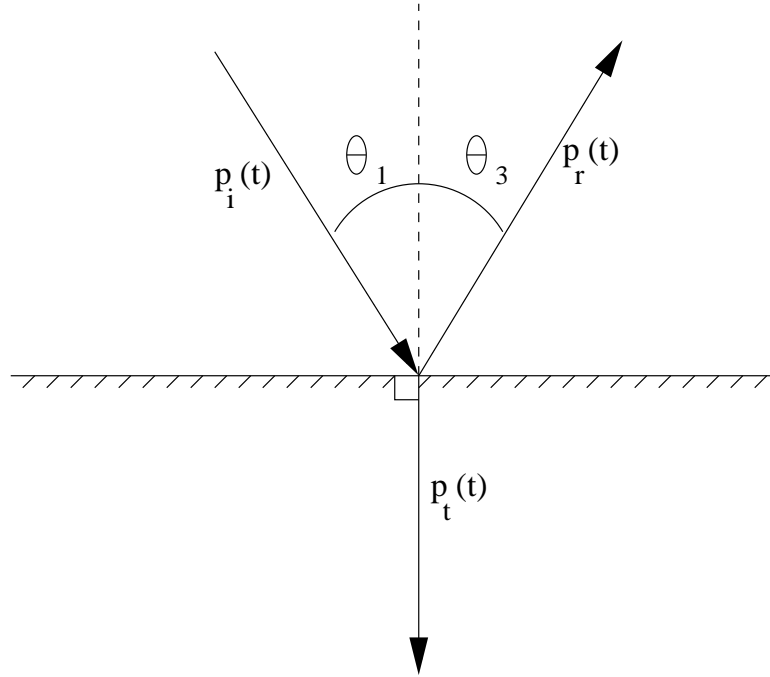


Figure 5: Reflection on a surface of locally reacting material

2.6 Absorption

Where reflection coefficient defines the ratio of amplitudes, the absorption coefficient relates to energies. And just like the reflection coefficient the absorption coefficient is a function of frequency and angle of incidence. The definition of the absorption coefficient is

$$\alpha(f, \theta) = 1 - |R(f, \theta)|^2, \quad (37)$$

where $R(f, \theta)$ is an angle- and frequency-dependent reflection coefficient.

2.7 Losses in the material

Just like in Equation (25), the propagating plane wave is in the form of $e^{-\gamma x}$, where $\gamma = jk$ is called the propagation constant. When the propagation constant is known the sound field can be solved anywhere in the material. Figure 6 illustrates a pressure wave traveling in a material. The wave number, k , is defined as

$$k = \frac{\omega}{c} = \omega \sqrt{\rho_0 Q}, \quad (38)$$

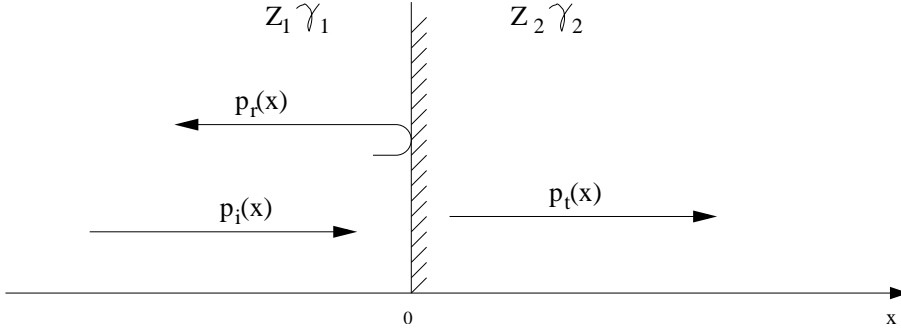


Figure 6: Losses in material

where Q is the bulk modulus and ρ_0 is the density. These values are complex, so the propagation is complex as well. The imaginary part determines the phase behavior of the wave and the real part accounts for the losses.

By using Equations (22) and (28), the impedance at any point can be written as

$$Z(x) = Z_1 \frac{e^{-\gamma x} + R e^{\gamma x}}{e^{-\gamma x} - R e^{\gamma x}}, \quad (39)$$

where x is the distance from the boundary. For normal incidence the reflection coefficient is defined as

$$R = \frac{Z_2 - Z_1}{Z_2 + Z_1}. \quad (40)$$

So Equation (39) can be written as

$$Z(x) = Z_1 \frac{e^{-\gamma x} + \left(\frac{Z_2 - Z_1}{Z_2 + Z_1}\right) e^{\gamma x}}{e^{-\gamma x} - \left(\frac{Z_2 - Z_1}{Z_2 + Z_1}\right) e^{\gamma x}} \quad (41)$$

After writing out the parenthesis and rearranging the terms the impedance can be written as

$$Z(x) = Z_1 \frac{Z_2(e^{-\gamma x} + e^{\gamma x}) + Z_1(e^{-\gamma x} - e^{\gamma x})}{Z_2(e^{-\gamma x} - e^{\gamma x}) + Z_1(e^{-\gamma x} + e^{\gamma x})}. \quad (42)$$

Because $\sinh(\alpha) = \frac{1}{2}(e^{\alpha} + e^{-\alpha})$ and $\cosh(\alpha) = \frac{1}{2}(e^{\alpha} - e^{-\alpha})$, the normal characteristic impedance can be written in the form of

$$Z(x) = Z_1 \frac{Z_2 \cosh(\gamma x) + Z_1 \sinh(\gamma x)}{Z_2 \sinh(\gamma x) + Z_1 \cosh(\gamma x)} \quad (43)$$

or

$$Z(x) = Z_1 \frac{Z_2 + Z_1 \tanh(\gamma x)}{Z_1 + Z_2 \tanh(\gamma x)}. \quad (44)$$

With these equations the impedance can be solved anywhere in the material. [29]

2.8 Impulse response measurement

An impulse response of a system characterize the system completely. The idea of the measurement is that when a known signal $x(t)$ goes through a system $h(t)$ which properties are known, the output $y(t)$ can be calculated by convolution. Convolution is defined as:

$$y(t) = x(t) * h(t) = \int_{-\infty}^{\infty} x(t)h(\tau - t)dt. \quad (45)$$

By taking the Fourier transform of above equation the convolution can be written in frequency domain as:

$$Y(f) = H(f)X(f), \quad (46)$$

where $Y(f)$, $H(f)$ and $X(f)$ are the Fourier transforms of $y(t)$, $h(t)$ and $x(t)$. Usually, the excitation signal $X(f)$ and the output $Y(f)$ are known and the properties of the material $H(f)$ should be found out. This can be achieved by deconvolution:

$$H(f) = \frac{Y(f)}{X(f)}, \quad (47)$$

where $H(f)$ is the impulse response of the system. By taking the inverse Fourier transform of the $H(f)$, the impulse response can be transformed back to time domain: $\mathcal{F}^{-1}H(f) = h(t)$. [16]

In this work all the impulse response measurements are performed by using a sweep-like excitation signal. Noise-like excitation signals, e.g., MLS are known have to have distortion artifacts due to the nonlinearities in the measurement system. To understand the benefit of a sweep like excitation signal one might first think of performing the measurement at a very small frequency band. If there is any harmonic distortion in the excitation signal, e.g., due to the nonlinearities in the loudspeaker, they will be out of the used frequency band and this way will not interfere the measurement. Now, this measurement can be swept over the whole frequency range and the harmonic distortion in the measurement data due to the nonlinearities in the system can be considerably decreased. [9, 29]

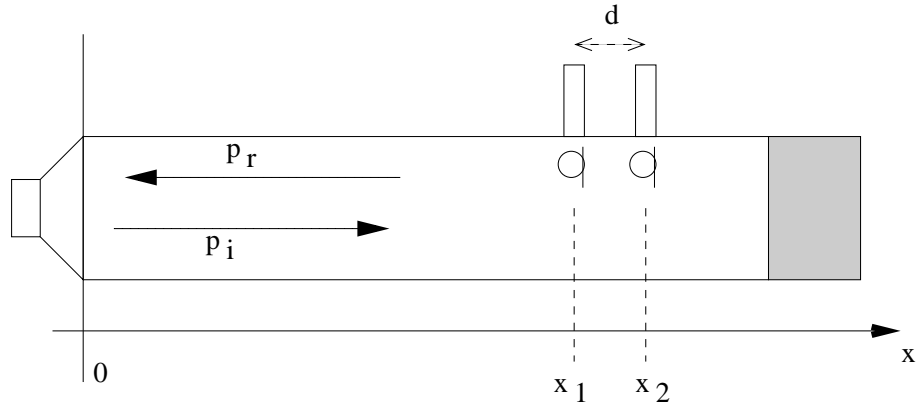


Figure 7: Kundt's impedance tube using the transfer function method

2.9 Laboratory measurements of acoustic materials

In a laboratory, the acoustic properties of materials are often measured by using the Kundt's impedance tube or by using the reverberation room method. These methods are also often referred to as reference methods.

2.9.1 Impedance tube method

In the impedance tube method, a small sample of the material is placed at the end of the tube and a sound source is placed at the other end. (See Figure 7.) There are two variations of the measurement procedure, the method of standing wave ratio and the transfer function method. In both cases, the properties of the materials are deduced by inspecting the incident and the reflected pressure plane waves inside the tube. In the transfer function method, the sound field is measured with two microphones. The properties are obtained by calculating the transfer function between the two microphones. With the standing wave ratio method the pressure maximum and minimum of the standing wave are searched for with a movable microphone. The measurement needs to be done separately at each frequency. This makes the standing wave ratio method fairly impractical and time consuming. Nowadays the impedance tube measurements are mainly done by using the transfer function method.

In the following the microphones are assumed to be calibrated. Normally the measurements should be compensated with a calibration measurement. The pressure waves inside the tube are assumed planes. This assumption sets the high frequency-limit for the measurement. For a round tube the high-frequency limit is set by

$$f_0 = 1.84 \frac{c}{\pi D}, \quad (48)$$

where D is the diameter of the tube.

The sound pressure field inside the tube is a combination of an incident and reflected wave. The sound pressures measured by the microphones are given by

$$p_1(x, f) = P_i(f)e^{-jkx_1} + P_r(f)e^{jkx_1}, \quad (49)$$

$$p_2(x, f) = P_i(f)e^{-jkx_2} + P_r(f)e^{jkx_2}, \quad (50)$$

and the transfer functions for incident and reflected waves are given by

$$H_i = \frac{P_i(f)e^{-jkx_1}}{P_i(f)e^{-jkx_2}} = e^{-jkd} \quad (51)$$

$$H_r = \frac{P_r(f)e^{-jkx_1}}{P_r(f)e^{-jkx_2}} = e^{jkd} \quad (52)$$

The reflected pressure wave p_r can be written as a product of the reflection coefficient $R(f)$ and the incident pressure wave p_i

$$p_r = R(f)p_i \quad (53)$$

The transfer function H_{12} between the microphones is defined as the ratio between $p_2(f)$ and $p_1(f)$. By substituting Equation (53) to Equations (49) and (50), H_{12} becomes

$$H_{12} = \frac{p_2(f)}{p_1(f)} = \frac{e^{jkx_2} + R(f)e^{-jkx_2}}{e^{jkx_1} + R(f)e^{-jkx_1}}. \quad (54)$$

Now the reflection coefficient $R(f)$ can be solved

$$R(f) = \frac{H_{12}(f) - e^{-jkd}}{e^{jkd} - H_{12}(f)} e^{2jkx_1}. \quad (55)$$

The surface impedance and absorption coefficients can be calculated by substituting Equation 55 to Equations (30) and (37). [17]

2.9.2 Reverberation room method

The impedance tube method assumes plane waves and measures impedance only at normal incidence. The size of the sample required for the impedance tube is in the order of a few centimeters and the method is not applicable for materials with surface structure bigger than the tube's diameter. These kinds of materials can be measured by

using the reverberation room method. The measurement is done in a special reverberation room. The sample size required in this method is in the order of from few to ten square meters. The reverberation room method gives only the absorption coefficient of the material.

The measurement is done (ideally) in diffuse field and this way the measurement conditions are closer to real life situations compared to tube measurements.

First, the reverberation time T_0 of the chamber is measured. The reverberation time is related to the absorption coefficient with the Sabine formula

$$T_0 = 0.163 \frac{V}{S\alpha_0}, \quad (56)$$

where V is the volume of the chamber, S is the wall area. $S\alpha = A$ is called the absorption area. Now the absorbent is brought to the chamber and once again the reverberation time T_1 is measured. By applying the Sabine formula the absorption area can be solved

$$A = A_1 - A_0 = 0.163V \left(\frac{1}{T_0} - \frac{1}{T_1} \right), \quad (57)$$

where A is the absorption area of the absorbent, A_0 is the absorption area of the chamber and A_1 is the absorption area of the chamber and the absorbent together. The absorption coefficient of the material can be calculated with

$$\alpha = \frac{A}{S}, \quad (58)$$

where S is the area of the absorbent. [17, 16]

3 In-situ measurements

3.1 Introduction

As laboratory measurements are done in a different place than where the actual material is normally placed, the measurement method could be called the *ex-situ* technique. On the other hand, doing the measurement *in-situ* means that the measurement is done in the place where the material really is. For example an absorbent on a concert hall wall would be measured in the concert hall.

In-situ measurements face many challenges that are not present in the laboratory environment. Maybe the most disturbing factors are the reflections from the surrounding surfaces. These parasitic reflections need to be filtered out somehow, and in a practical way this is done, e.g., by truncating the temporal response. Due to the lack of required technology this was not possible until the 1970's. Since then there has been numerous propositions for in-situ measurement techniques.

However, a proper method covering the whole frequency range of interest, e.g. in building acoustics (50 Hz - 5 kHz), is still missing. Especially at low frequencies measuring below 200 Hz seems to be really difficult. The required windowing sets the theoretical low frequency limit and also at such low-frequencies the wavelengths are so long that the assumptions made for the measurement don't hold anymore.

The in-situ measurement techniques can be roughly divided into two main groups: the windowing and the free-field methods. In the first method the incident and the reflected sound are separated somehow, e.g. by windowing. By comparing the sounds the absorption can be obtained. In the second group the direct and the reflected sound are left to combine and the impedance is calculated from the resulting interference patterns.

One of the first in-situ measurement techniques was proposed by Ingård and Bolt [12] in 1951. It was a free-field method where first a reference measurement was performed at the surface of a hard and ideally reflecting material. Then the measurement was repeated in front of an absorbent. By comparing the measurements the properties of the material could be obtained. Due to the lack of required technology the method could not however be used in-situ at that time but later there has been many methods based on it [24, 25, 26]. Klein and Cops [15] proposed a standing wave ratio based free

field method for measuring the surface impedance at oblique incidence. This method is basically the same as the traditional Kundt's impedance method with a movable microphone. The measurement is done in two or more different places in front of the material to find the pressure maximum and the minimum of the standing wave. From this data the properties of the material can be calculated.

In the free-field methods the two-microphone version seems [1, 2, 8, 11] to be more popular and applicable. Just like in the impedance tube transfer function method the measurement is done with two microphones in front of the material. From the transfer function between the two microphones the acoustical properties at the surface can be solved. One clear advantage of using two microphones is that the surrounding noise can be canceled out more efficiently compared to methods using only one microphone.

The traditional windowing method [10, 19] is a very straightforward measurement technique. It is basically just an impulse response measurement in front of the surface, and the incident and the reflected waves are separated by windowing. There are two major concerns in this method. The impulses should not interleave so the impulses should be short and they should be clearly separated in time. The same papers also suggest using pre-emphasized excitation signal to shorten the impulses. When the excitation signal is inverse filtered with the measurement system impulse response, the impulse response can be shortened considerably. The second concern is that because the impulses need to be windowed out from an already windowed data, the low frequency resolution is very poor in this technique.

To maximize the usage of the time window Mommertz [20] suggested a subtraction method for canceling the direct sound in the impulse response. In the subtraction method a reference measurement is done far away from reflecting surfaces. If the loudspeaker-microphone distance is kept the same and the measurement is repeated in front of the material, the direct sounds should be identical in the reference and in the material measurement. When the reference measurement is subtracted from the reflection measurement the direct sound can be canceled out. This allows taking the measurement device close to the surface because it doesn't matter if the impulses interleave. But then again, the measurement device comes also closer to the surface and causes parasitic reflection which degrades the measurement data. These reflections are so close in time that windowing these out would degrade the low-frequency resolution considerably. Karjalainen and Tikander [14] suggested using a hard surface measurement as a reference to reduce the effect of these parasitic reflections from the loudspeaker. In addition to the reference and material measurement, another measurement is performed in front of a hard surface. If the measurement is done at the same distance as the material measurement, the parasitic reflections from the loudspeaker should be temporally located in the same place in the impulse response in both measurements. If the material measurement is compared to the hard surface measurement the effect of the parasitic reflection can be reduced.

Most of the in-situ measurement techniques rely on the plane wave assumption. In the far field, when the distances are much longer than the wave length the plane assumption holds fairly well. But in in-situ conditions, especially at low frequencies, the far field requirement is practically impossible to fulfill. There are a lot of studies how and in what condition the plane wave assumption can be used [2, 15, 23, 28]. Especially, Nobile and Hayek [23] have done a deep research on how acoustical waves propagate over a boundary and how this corresponds to the plane wave assumption. As a general rule, when the wavelength is small compared to the measurement dimensions and when using small angles (compared to normal incidence), the plane wave assumption can be safely used. Probably the biggest reason for using the plane wave assumption is simplicity. With plane waves the acoustic sound fields can be solved analytically and the measurement can be done even with modest computational power. On the other hand, with modern efficient computers the acoustical fields with spherical waves can be solved numerically [2, 5, 23] and this way the accuracy at oblique incidence and at low frequencies can be increased considerably.

One feature that is not always controllable in in-situ situations is the size of the sample under study. Most of the proposed techniques assume that the measurement area is infinite, or at least large compared to the wavelength. According to Nocke [25] the sample size should cover first few Fresnel zones. Here a Fresnel zone means a reflected path length in wavelengths from source to receiver. Clearly for low frequencies, the sample size should be several square meters. Nocke doesn't give any exact results how much the sample size affects the results but in general, too small samples will underestimate absorption values. Allard and Sieben [1] proposed using the transfer function method to measure small sample sizes. If the microphones are taken very close to the surface, the surrounding areas won't affect the intensity at the place of the measurement. Because the microphones need to be very close to the surface, also the distance between microphones is small. For this reason the method is applicable only at frequencies above 500 Hz. When considering the sample the main question is, are we measuring the properties of the material or the properties of the whole surface structure.

Most of the restrictions mentioned above are hard or impossible to overcome. For example, the frequency resolution due to the windowing is the theoretical limit for low frequencies. Karjalainen and Tikander [14, 30] suggested using acoustical models to increase the robustness of the measurement, especially at low frequencies. If the basic behavior of a surface structure is known, a model could be created and fitted to the measurement data. This way the measurement range could be extended to the areas where the actual measurement method doesn't apply or the environment restricts the measurements. The downside of the method is finding proper models and especially models with few parameters.

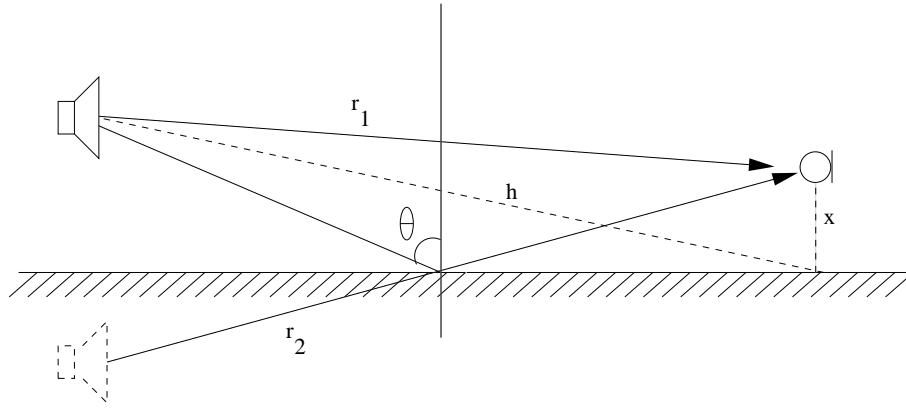


Figure 8: Measurement of absorption coefficient with one microphone by using the free field method.

3.2 Free-field method

In the free field measurement techniques the incident and the reflected waves are left to combine. The acoustical properties are calculated from the interference pattern in front the surface. Most of the in-situ free methods are fairly straight analogies from the traditional laboratory measurement techniques. In the following two methods are presented. The first one is a one microphone method based on studying the standing wave ratio in front of the surface. The second one is a two microphone transfer function method.

3.2.1 One microphone

When a point source is continuously emitting sound of one frequency the resulting sound field is a combination of the direct and the reflected sound. (See Figure 8.) When assuming plane waves the sound pressure at the receiver can be written as

$$p = \frac{e^{ikr_1}}{r_1} + R \frac{e^{ikr_2}}{r_2}, \quad (59)$$

where R is reflection coefficient. For small receiver heights ($x \ll h$) the following approximation can be used:

$$r_1 = h - x \cos \theta \quad (60)$$

$$r_2 = h + x \cos \theta \quad (61)$$

$$\left(1 - \frac{x}{h} \cos \theta\right)^{-1} = e^{\frac{x}{h} \cos \theta} \quad (62)$$

$$\left(1 + \frac{x}{h} \cos \theta\right)^{-1} = e^{-\frac{x}{h} \cos \theta} \quad (63)$$

Now Equation (59) can be rewritten

$$p(x) = \frac{e^{ikh}}{h} \left(e^{-ikx \cos \theta + \frac{x}{h} \cos \theta} + R e^{ikx \cos \theta - \frac{x}{h} \cos \theta} \right), \quad (64)$$

where $R = -e^{-2\psi}$ is the reflection coefficient. As $u_n(x) = p(x)/\rho c$, the normal surface impedance $Z_n(x)$ can be written as

$$Z_n(0) = \frac{p(0)}{u_n(0)} = \frac{\rho c}{\cos \theta \left(1 + \frac{j}{kh}\right)} \tanh \psi, \quad (65)$$

where $\tanh \psi = u + jv$. u and v can be calculated as functions of the distance to the first pressure minimum and the standing wave ratio:

$$u = \frac{1}{2} \ln \left[\frac{e^{-d_1 \cos \theta/h} + s e^{-d_2 \cos \theta/h}}{e^{d_1 \cos \theta/h} - s e^{d_2 \cos \theta/h}} \right], \quad (66)$$

$$v = \pi + kd_1 \cos \theta, \quad (67)$$

where d_1 is the first pressure minimum, d_2 is the following pressure maximum and s is the standing wave ratio. The term d_2 can be calculated when d_1 is known

$$d_2 = d_1 + \frac{\pi}{2k \cos \theta}. \quad (68)$$

The standing wave ratio s is defined as

$$s = \frac{|p_{\min}|}{|p_{\max}|}. \quad (69)$$

If the reflection coefficient is R the pressure at the maximum is $|p_{\max}| = |p_i|(1 + |R|)$ and at the minimum $|p_{\min}| = |p_i|(1 - |R|)$, where p_i is the incident pressure wave. The maximum occurs when the incident and the reflected waves are in phase, and the minimum when the waves are out of phase. Now s can be written as

$$s = \frac{1 - |R|}{1 + |R|}. \quad (70)$$

From Equation (70), the absolute value of the reflection coefficient can be solved

$$|R| = \frac{1 - s}{1 + s}. \quad (71)$$

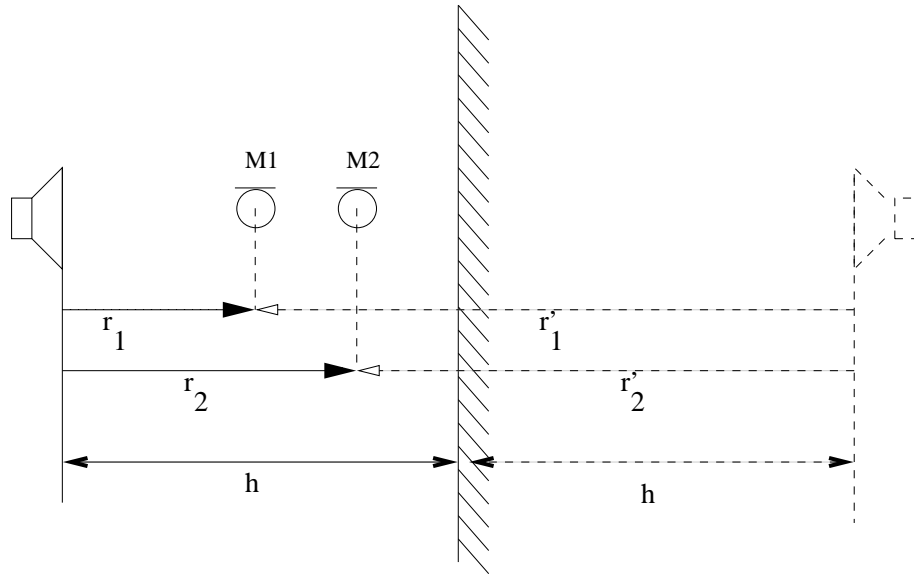


Figure 9: Measurement of absorption coefficient with two microphones by using the free field method.

Because the place of the pressure minimum is known, the phase of the reflection coefficient can be written as

$$\phi = \frac{4\pi d_1}{\lambda}, \quad (72)$$

where λ is the wavelength. Now the complex reflection coefficient can be written as:

$$R = |R|e^{j\phi} \quad (73)$$

The reflection coefficient measurement needs to be done at one frequency at time and at each frequency the first pressure minimum has to be searched for. This makes the measurement rather impractical and time consuming.

3.2.2 Two microphones

Just like with the impedance tube measurements the two microphone transfer function method provides a more practical solution for measuring the surface impedance. The measurement can be done by using an excitation signal having a wide frequency band, e.g., white noise and only one or two measurements are needed to cover the whole frequency range. The in-situ measurement is analogous to the impedance tube measurement.

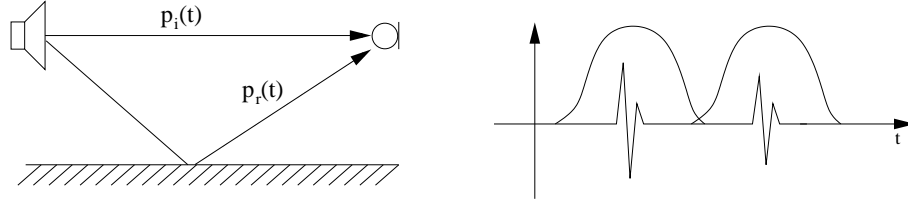


Figure 10: Measurement of surface impedance by using the windowing method

Looking at the measurement setup in Figure 9, the pressures at the microphones M1 and M2 can be written as:

$$p_{M1}(x) = \frac{e^{jkr_1}}{r_1} + R \frac{e^{jkr'_1}}{r'_1} \quad (74)$$

and

$$p_{M2}(x) = \frac{e^{jkr_2}}{r_2} + R \frac{e^{jkr'_2}}{r'_2}. \quad (75)$$

The transfer function $H(\omega)$ can now be written as

$$H(\omega) = \frac{p_{M2}(x)}{p_{M1}(x)} = \frac{\frac{e^{jkr_2}}{r_2} + R \frac{e^{jkr'_2}}{r'_2}}{\frac{e^{jkr_1}}{r_1} + R \frac{e^{jkr'_1}}{r'_1}}. \quad (76)$$

$H(\omega)$ can be measured and thus the reflection coefficient R can be solved as

$$R = \frac{\frac{e^{jkr_2}}{r_2} + H(\omega) \frac{e^{jkr'_2}}{r'_2}}{\frac{e^{jkr_1}}{r_1} + H(\omega) \frac{e^{jkr'_1}}{r'_1}}. \quad (77)$$

The spacing between the microphones sets the frequency limits for this method. When the distance between the microphones is increased the high-frequency limit will drop but the sensitivity at low frequencies will increase and vice versa.

3.3 Windowing method

In the windowing method the impulse response is measured in front of the material under study. Then the direct and the reflected sounds are separated from the impulse response by windowing, see Figure 10. The length of the window sets the frequency resolution for the measurement. If the length of the window is T , then the obtained frequency resolution is $1/T$ [17]. In normal rooms this results in a fairly high low-frequency limit.

After windowing there are two separate impulse responses: the direct sound $p_i(t)$ and the reflected sound $p_r(t)$. The corresponding Fourier transforms are $P_i(f)$ and $P_r(f)$. Then the reflection coefficient is

$$R(f) = \frac{P_r(f)}{P_i(f)} \quad (78)$$

The amplitudes of the windowed signals need to be corrected according to the spherical attenuation law.

The measurement needs to be done fairly far from the surface in order to keep the impulses apart from each other. In this way the impulses will distort each other as little as possible.

To increase the signal separation, Mommertz [19] proposed using pre-emphasized pseudo-noise as an excitation signal. The pre-emphasis is used to flatten the loudspeaker's frequency response and this then shortens the impulse of the direct sound. To create the pre-emphasis filter, the impulse response of the system is measured. Then the inverse of the system response is used to filter the excitation signal. This way the pulses in the impulse response can be shortened maximally.

3.4 Subtraction method

The subtraction method was initially proposed by Mommertz in 1995 [20]. It is a variation of the windowing method and it improves the low-frequency resolution considerably.

The impulse response of the loudspeaker is first measured in free field. As a result the transform gives a slightly delayed impulse response $h_d(t)$ of the loudspeaker and the whole measuring system (see Figure 11(a)). The delay is due to the sound wave traveling from loudspeaker to the microphone.

Now, the same measuring system is taken close to a surface, as shown in Figure 11(b), and the measurement is repeated. In an ideal case and if the loudspeaker-microphone distance is kept the same, exactly the same direct sound impulse is produced as in the free field case. But now there is also another impulse, which is the reflection from the surface. Figure 11(b) shows also the impulse response $h_r(t)$ of the reflection measurement. Naturally, because the measurements are done in real space there are also other surfaces causing parasitic reflections. These must be windowed out.

By subtracting the free field measurement from the reflection measurement, $h_r(t) - h_d(t)$, an impulse response $h(t)$ which has only the reflection is produced (Figure 11(c)). The impulse response $h(t)$ has also the phase information of the reflection.

Next the impulse responses $h_d(t)$ and $h(t)$ are Fourier transformed yielding $H_d(f)$ and

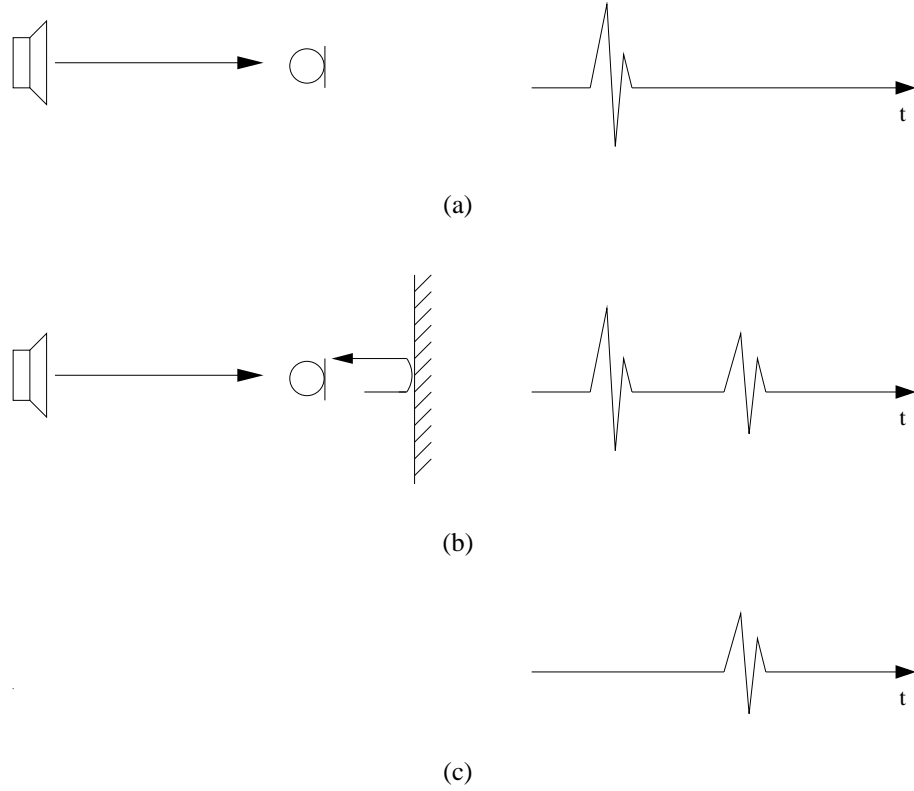


Figure 11: Measurement of surface impedance by using the subtraction method and impulse responses schematically. (a) Reference measurement and impulse response $h_d(t)$. (b) Measurement in front of material and impulse response $h_r(t)$. (c) Impulse response $h(t) = h_r(t) - h_d(t)$ after subtraction.

$H(f)$. The latter spectrum also includes the measuring system response so it needs to be compensated with the free field response. Before the compensation can be done the amplitudes of the impulses must be matched. The reflected impulse has decreased in amplitude according to the spherical wave attenuation law. This can also be done later in the frequency domain. Now the complex reflection coefficient $R(f)$ can be calculated:

$$R(f) = \frac{H(f)}{H_d(f)}. \quad (79)$$

From the complex reflection coefficient, the specific impedance of the surface can be deduced by

$$\zeta(f, \theta) = \frac{1}{\cos \theta} \frac{1 + R(f, \theta)}{1 - R(f, \theta)}, \quad (80)$$

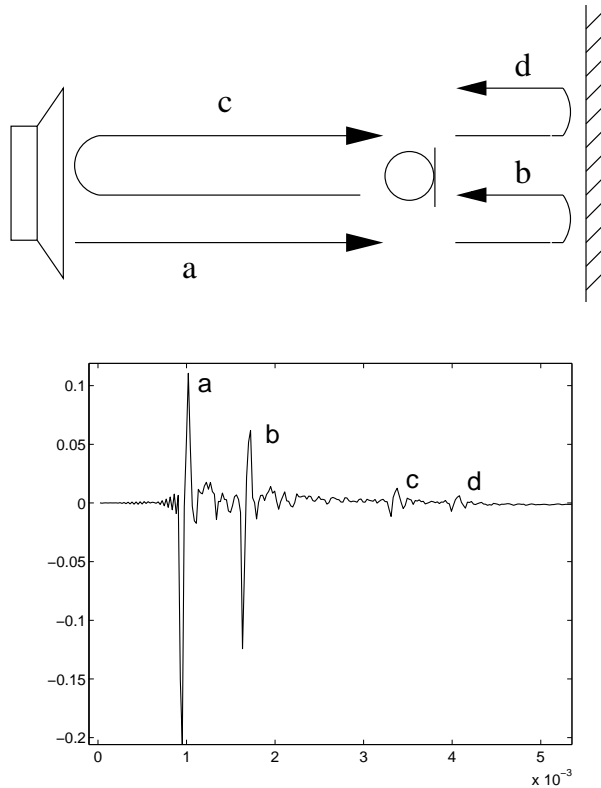


Figure 12: Top: Schematical drawing on how the pulses are formed in an impulse response measurement a) direct sound b) reflection from the surface c,d) parasitic reflections from the loudspeaker. Bottom: A measurement performed in front of a concrete floor.

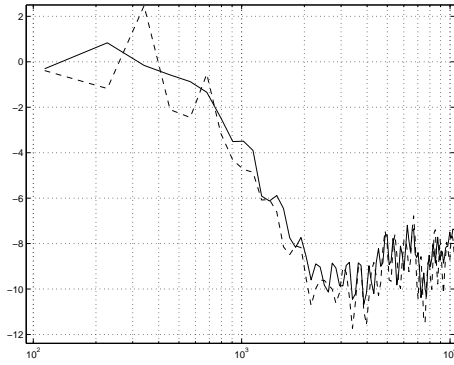
where θ is the angle of incidence. The absorption coefficient is given by

$$\alpha(f, \theta) = 1 - |R(f, \theta)|^2. \quad (81)$$

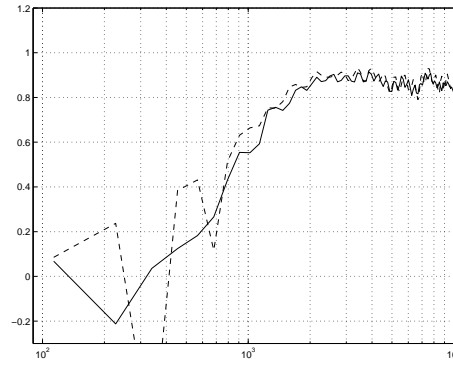
3.4.1 Using hard surface as reference

If the source is relatively close to the surface, the parasitic reflections from the loudspeaker degrade the measured impulse response (see Figure 12.) The parasitic reflections cannot be windowed out because they are so close in time to the actual reflection. Figure 12 shows a measurement performed in front of a concrete floor. The parasitic reflections result in comb filter like fluctuation in the frequency response. Figure 13 shows the fluctuation in a real life measurement data.

The effect of the reflections can be decreased by using a so called hard surface mea-



(a) Reflection coefficient



(b) Absorption coefficient

Figure 13: Reflection and absorption coefficients measured by using the subtraction technique. Dashed line is without and solid line is with the hard surface reference. (18 mm rock wool, density 40 kg/m².)

surement as a reference. In addition to measurements shown in Figure 11 a third measurement is done in front of a hard surface. The direct sound is subtracted the same way as in the material measurement. The resulting impulse in the response should be (ideally) identical to the reference measurement, except that the impulse is delayed and less in amplitude due to the longer traveling distance. But now this response has also the same parasitic reflection from the loudspeaker as the material measurement. If the hard surface measurement is done at the same distance as the material measurement, the parasitic reflections should be at the same place in time.

Now the material measurement is compared to the hard surface measurement. The fluctuations due to the parasitic reflections should be canceled out. Figure 13 shows the improvement in the measurements. Especially at low frequencies the fluctuation has decreased effectively. However, the absorption coefficient still has some negative values which are physically impossible for passive materials. So, even though the method gives smoother responses, the results should be used with care.

4 Error sources in measurements

4.1 The plane wave assumption

Many of the in-situ measurement methods rely on a plane wave assumption. As already stated in chapter 2.3.1, the pressure field close to a surface can be written with so called Weyl-van der Pol equation:

$$p = \frac{e^{jk_1 r_1}}{r_1} + \frac{e^{jk_1 r_2}}{r_2} [(1 - R)F + R], \quad (82)$$

where R is a plane wave reflection coefficient and F is a correction term that accounts for the sphericity of wave fronts. At small wavelengths ($\lambda \ll r$) and with small angles of incidence F approaches zero and Equation (82) approaches the plane wave approximation given in Equation (33).

Nobile and Hayek [23] have introduced an exact solution for Equation (82) and compared the results with plane wave approximation. The exact form of term F in Equation (82) is written as

$$F = 1 + i2(w)^{\frac{1}{2}} e^{-w} \int_{-i(w)^{1/2}}^{\infty} e^{-u^2} du, \quad (83)$$

where u is particle velocity and

$$w = i \frac{4k_1 r_2}{(1 - R)^2} \frac{Z_1^2}{Z_2^2} \left(1 - \frac{k_1^2}{k_2^2} \cos^2 \psi\right), \quad (84)$$

where Z is acoustic impedance, k is wave number and ψ is an angle of incidence, as shown in Figure 14. The derivation of an exact solution for Equation (82) will not be shown here (see reference [23] for details) but it will only be noted that the solution can be written as an asymptotic Taylor series. In the following the exact (numerical) solution is compared to a plane wave approximation, where F is assumed zero. The results in Figures 15 and 16 are by Nobile and Hayek [23].

The comparison is performed in terms of an excess attenuation, which is defined as

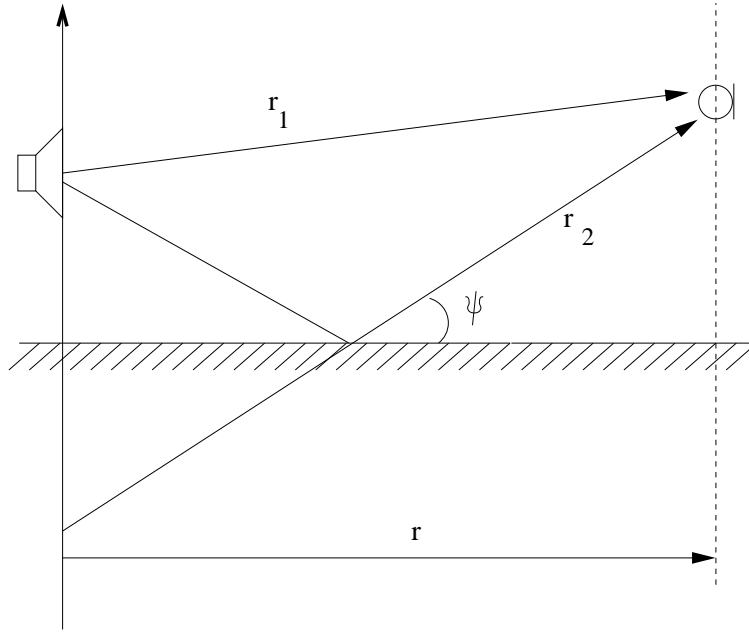


Figure 14: Geometry of the spherical propagation problem

$$attenuation = -20 \log_{10} \left| \frac{p_{tot}}{p_{dir}} \right| \text{ dB}, \quad (85)$$

where p_{tot} is the total pressure field at the receiver, and p_{dir} is the direct field only. The excess attenuation will be presented as a function of kr_2 . By using Equation (19) the value of kr_2 can be translated to frequencies:

$$f = \frac{kr_2c}{2\pi r_2}, \quad (86)$$

where r_2 is the length of the traveling path from source to receiver for the reflected wave.

Figure 15 shows numerical results for a case with very small angle of incidence ($\psi = 3^\circ$) for materials with low and a bit higher characteristic impedance. (Note that the angle is defined in a different way from previous discussion.) It can be seen that with very oblique angle of incidence the plane wave assumption gives very erratic results, even with very high values of kr_2 . With a material having low characteristic impedance (Figure 15(a)) the plane wave approximation gives same results with the exact solution when kr_2 is higher than 100. This corresponds to frequencies above 410 Hz.

Figure 16 shows the numerical results for a case with larger angles of incidence. For the case in Figure 16(a) the angle of incidence is 45° and $r_2 = 13.2$ m. Now it can be

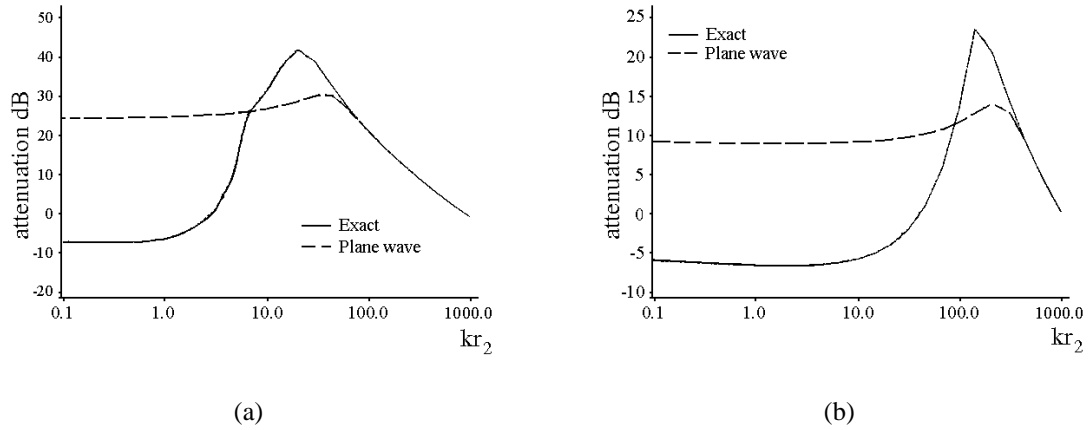


Figure 15: Excess attenuation as a function of kr_2 at a small angle of incidence. The specific impedance of the ground is a) $\zeta = 0.3 + j0.5$ b) $\zeta = 2.0 + j3.0$. For both cases $r_2 = 13.2$ m and $\psi = 3^\circ$.

seen that the plane wave approximation doesn't differ so much from the exact solution anymore. The plane wave approximation seems to be fairly accurate when kr_2 is higher than 5. This corresponds to frequencies above 20 Hz. Figure 16(b) shows a case with normal incidence but now r_2 is only 1.4 m. The plane wave approximation meets the exact solution at about $kr_2 = 10$ and this corresponds to a frequency of 390 Hz.

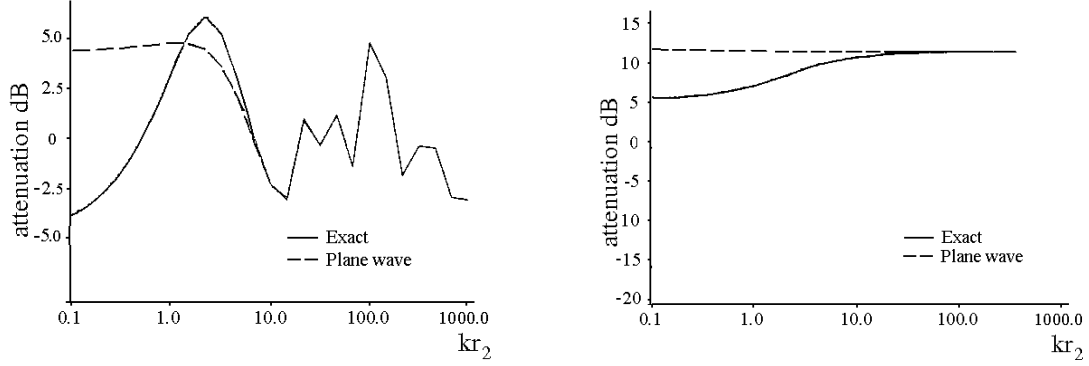
So, it can be clearly seen that when the measuring distance is kept long enough and the angle of incidence large enough the plane wave approximation can be used.

4.2 Parasitic reflections from the source

When the measurement device is taken close to the surface under study, the loudspeaker will cause parasitic reflections, which will degrade the measurement data. Figure 17 shows how the parasitic reflections are formed.

The second order reflections from the source are so close in the time domain that they cannot be removed by truncating the temporal response. Figure 18(b) shows how the reflections are located temporally. The impulse measurement was performed in front of a concrete floor. The microphone was 122 mm from the floor and 300 mm from the loudspeaker. It can be seen in the impulse response that the temporal distance between the actual impulse from the first parasitic reflection is only 1.7 ms. By windowing the actual impulse out of the response would result in a really poor low frequency resolution.

Figure 18 shows the effect of the parasitic reflections. In Figure 18(a) an ideal impulse is added with extra impulses to simulate the second order reflections from the source.



(a) $\psi = 45^\circ, r_2 = 14.8 \text{ m}$

(b) $\psi = 90^\circ, r_2 = 1.4 \text{ m}$

Figure 16: Excess attenuation as a function of kr_2 at a small angle of incidence. The specific impedance of the ground is a) $\zeta = 0.3 + j0.5$ b) $\zeta = 2.0 + j3.0$.

Without the extra impulses the magnitude spectrum would be flat but the extra taps in the response result in a comb filter like magnitude spectrum. Figure 18(b) shows an actual measurement in front of a hard concrete wall. The direct sound is canceled by using the subtraction method.

The first parasitic reflection can be written as

$$p_{r1} = \frac{RR_m e^{jk(2r_1+r_m)}}{2r_1 + r_m}, \quad (87)$$

where R_m and R are the reflection coefficients of the loudspeaker and the surface, r_1 is the distance between the loudspeaker and the surface and r_m is the distance between the loudspeaker and the microphone. The second parasitic reflection can be written as

$$p_{r2} = \frac{R^2 R_m e^{jk(3r_1+r_w)}}{3r_1 + r_w}, \quad (88)$$

where r_w is the distance between the surface and the microphone. If the microphone is located close to the surface p_{r1} and p_{r2} can be simplified to

$$p_{r1} \approx \frac{RR_m e^{jk(3r_1)}}{3r_1} \quad (89)$$

$$p_{r2} \approx \frac{R^2 R_m e^{jk(3r_1)}}{3r_1}. \quad (90)$$

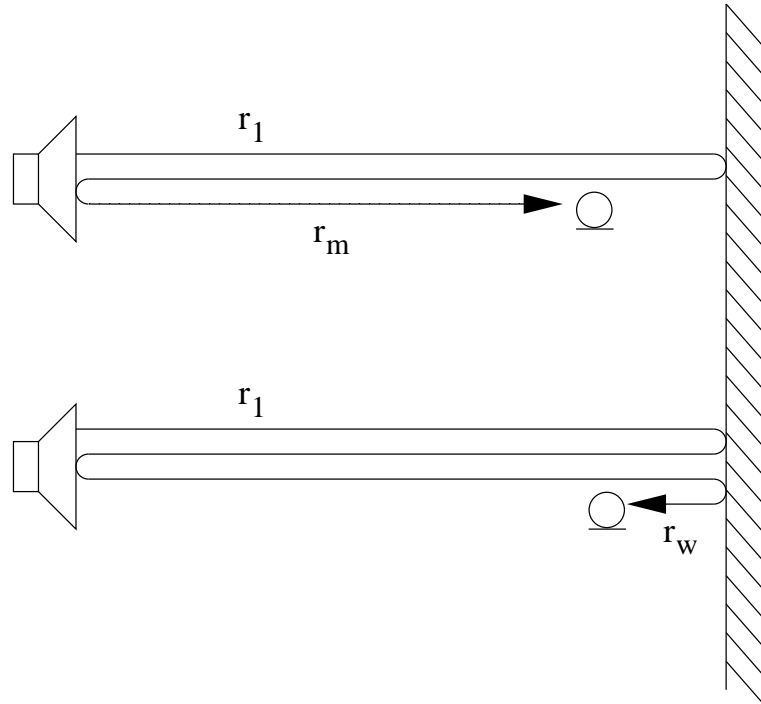


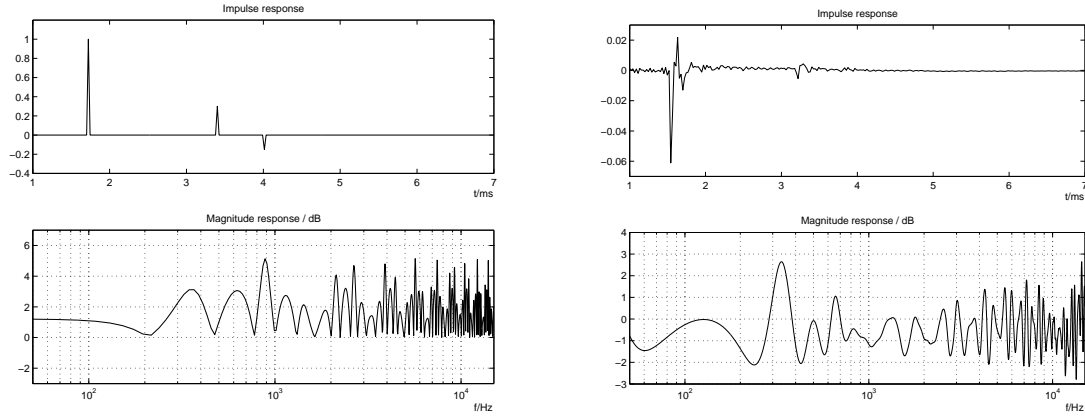
Figure 17: Formation of the second order reflections in in-situ measurements.

As it can be seen from Equations (89) and (90) that the effect of the parasitic reflections can be decreased by taking the loudspeaker further away from the surface, thus increasing r_1 and by minimizing R_m . With highly absorbing materials R will be small and also the effect of the reflections will be less disturbing.

4.3 Source directivity

In all of the in-situ measurement methods the measurement device consists of a loudspeaker and one or more microphones. In most cases, both of these are assumed to be omni-directional. The directionality of a loudspeaker or a microphone is proportional to the dimensions of the device. Modern microphones can be made so small (only few millimeters) that they are almost ideally omni-directional even up to 10 kHz. With loudspeakers, the size is a compromise between the directionality and sensitivity at low frequencies. The bigger the driver, the more sensitive the loudspeaker is at low frequencies but then the corner frequency where the loudspeaker starts to direct the sound comes lower. Figure 19 shows the directivity of the loudspeaker used in this work.

Let us consider the measurement setup in Figure 20. $H_0(f)$ is the sound pressure wave emitted toward the microphone and $H_\theta(f)$ is the sound pressure wave emitted



(a) An ideal impulse response with two simulated reflections

(b) A measured impulse response in front of a hard surface with parasitic reflections from the source. Microphone distance from the floor is 122 mm.

Figure 18: Effect of the parasitic reflections in the magnitude response.

toward the surface at an angle of θ . If the loudspeaker is not omni-directional then $H_0(f) \neq H_\theta(f)$ and this results in error in the calculations.

The effect of the directionality can be compensated if the directional pattern of the loudspeaker is known. The difference between the sound pressure spectra between the direct and oblique sounds is

$$H_c(f) = H_\theta - H_0(f). \quad (91)$$

With $H_c(f)$ the effect of the directionality of the loudspeaker can be compensated out:

$$H'_\theta(f) = \frac{H_\theta(f)}{H_c(f)}. \quad (92)$$

Now, for the reflected pressure wave H'_θ is used instead of H_θ . The compensation needs to be done at each angle separately.

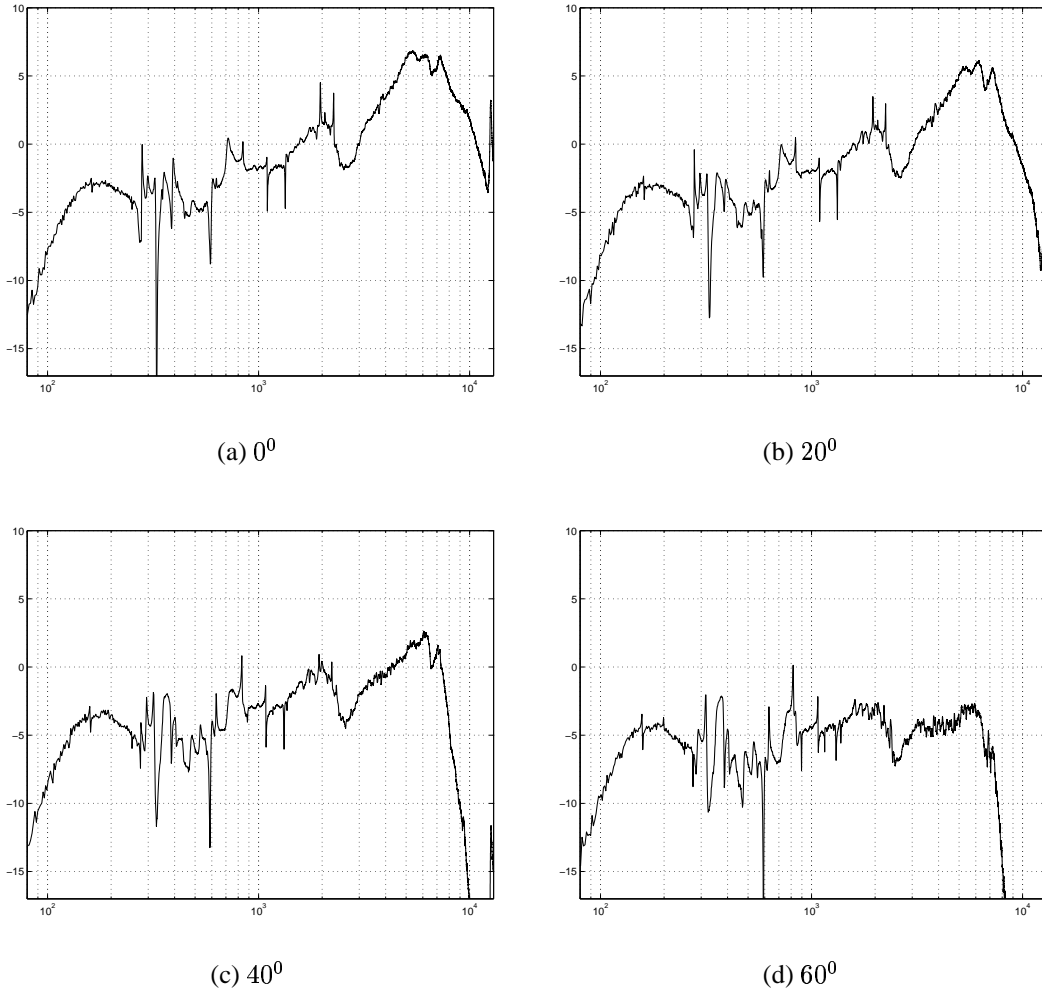


Figure 19: Frequency response of the loudspeaker used in this work in different directions.

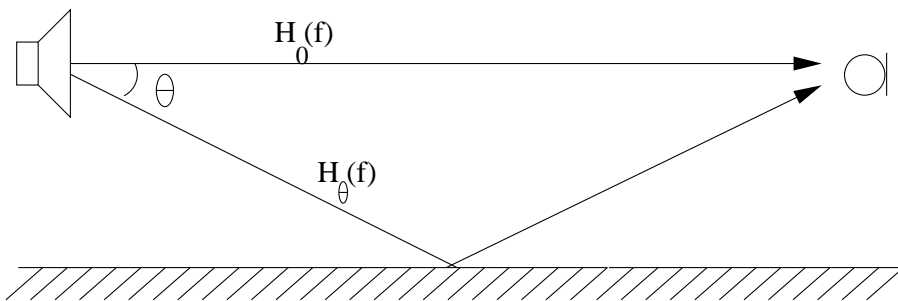


Figure 20: Error in the measurement due to the directivity of the loudspeaker

5 Model-based curve fitting

5.1 Introduction

Using the traditional measuring methods, Kundt's tube or reverberation room, on site may sometimes be very unpractical if not close to impossible. This is where in-situ methods come handy. There exist numerous methods for in-situ techniques, as already introduced in chapter 3. However, in-situ measurement methods still yield rather rough results. Especially at low frequencies none of the methods give reliable results.

If there were, and quite often there is information about the structure of surface under study, an acoustic model of the surface can be formed. This model can be used to increase the reliability of any in-situ measurement technique. By using some sophisticated curvefitting algorithm the model can be fitted to measurement data. This way the measurement can be proof-checked, and if the model is valid, the validity of the measurement could perhaps be extended to lower frequencies.

For curvefitting purposes the models should have as few parameters as possible, ideally just one or two. As a simple example one might consider a homogeneous wool-like absorbent on a hard surface. The reflection from the surface could be modeled with a simple low-pass filter with two parameters: cutoff frequency and high-frequency gain. Although, this model doesn't have a direct physical background it still nicely models the behavior of the system. As an application, a large number of different wool-like absorbents could be listed with just these two parameters.

There are also many kinds of empirical and semi-empirical, as well as purely theoretical models for acoustical wave propagation in materials. The major drawback in most of the models is that there are too many parameters for curvefitting. In 1970 Delany and Bazley [7] published empirical equations for the propagation coefficient γ and the characteristic impedance Z_0 in fibrous absorbents. The only parameter to measure was the flow resistivity R_f . Later, there has been many variations of the equations [18][3].

In the following chapters the Delany-Bazley model is introduced and tested. Also some variations for the Delany-Bazley models by Mechel [18] and by Allard and Champoux [3] are introduced. They add the validity of the models for different types of materials and increase accuracy at lower frequencies.

5.2 Acoustic wave propagation models

When the propagation constant γ and the characteristic impedance Z_c of the materials are known the acoustic wave behavior can be completely solved anywhere in the material. The following acoustic wave propagation models estimate these parameters and the only quantity to be known a priori for these models is the flow resistivity R_f . Of course this is hard to measure in-situ but R_f can be used as a free parameter in model-based curve-fitting.

5.2.1 Delaney-Bazley

In 1970 Delany and Bazley [7] made extensive measurements on a large number of different fibrous absorbents. By using regression analysis the empirical laws to estimate the propagation constant γ and characteristic impedance Z_0 were derived from measurement data. The equations for γ and Z_0 are given as:

$$\gamma = j \frac{\omega}{c} \left[1 + 0.0978 \left(\frac{\rho_0 f}{R_f} \right)^{-0.700} - j 0.189 \left(\frac{\rho_0 f}{R_f} \right)^{-0.595} \right], \quad (93)$$

$$Z_0 = \rho_0 c \left[1 + 0.0571 \left(\frac{\rho_0 f}{R_f} \right)^{-0.754} - j 0.0870 \left(\frac{\rho_0 f}{R_f} \right)^{-0.732} \right], \quad (94)$$

where R_f is flow resistivity.

The measurements were done by using impedance tube, therefore the model assumes plane waves and normal incidence. The model also assumes that the absorbent material is fibrous and the fibers are uniformly distributed in the material.

With the above assumptions the model is theoretically valid when the frequency dependent parameter $0,001 < \rho_0 f / R_f < 1,0$.

5.2.2 Mechel

Mechel [18] made also a large number of measurements on different kinds of absorbent materials and as a result derived equations for propagation constant and for characteristic impedance. These models merely just fine-tuned the models introduced by Delany and Bazley. The equations for γ and Z_0 are written as:

$$\gamma = j \frac{\omega}{c} \left[a' \left(\frac{\rho_0 f}{R_f} \right)^{-\alpha'} - j \left(1 + a'' \left(\frac{\rho_0 f}{R_f} \right)^{-\alpha''} \right) \right]. \quad (95)$$

$$Z_0 = \rho_0 c \left[1 + b' \left(\frac{\rho_0 f}{R_f} \right)^{-\beta'} - j \beta'' \left(\frac{\rho_0 f}{R_f} \right)^{-\beta''} \right]. \quad (96)$$

The model varies depending on the value of the parameter $(\rho_0 f / R_f)$. Table 1 shows the values for the parameters in the models.

Table 1: Parameters for the Mechel model

$\frac{\rho_0 f}{R_f}$	a'	α'	a''	α''	b'	β'	b''	β''
≤ 0.025	0.396	0.458	0.135	0.646	0.0668	0.707	0.196	0.549
> 0.025	0.179	0.674	0.102	0.705	0.0235	0.887	0.0875	0.770

For locally reacting materials the wave propagation in the material was always assumed to be normal to the surface. The Mechel model also applies for materials with extended reaction. This means that the acoustic wave in the material can also have a parallel component. This model is also found to be more accurate at low frequencies.

5.2.3 Allard-Champoux

In 1992 J. Allard and Y. Champoux [3] proposed equations for sound propagation in rigid frame fibrous materials. The equations provide more physical results at low frequencies compared to the equations presented by Delany and Bazley or Mechel.

The equations for the propagation constant $\gamma(\omega)$ and for the characteristic impedance $Z_0(\omega)$ are given by:

$$\gamma(\omega) = j2\pi f \sqrt{\frac{\rho(\omega)}{K(\omega)}} \quad (97)$$

$$Z_0(\omega) = \sqrt{\rho(\omega)K(\omega)}, \quad (98)$$

where $\rho(\omega)$ is the dynamic density and $K(\omega)$ is the dynamic bulk modulus. The dynamic density takes into account the inertial and the viscous forces per unit volume of the air in the material. The dynamic bulk modulus relates the divergence of the averaged molecular displacement of the air to the averaged variation of the pressure. The $\rho(\omega)$ and $K(\omega)$ are given by

$$\rho(\omega) = \rho_0 \left[1 + \frac{1}{i2\pi} \left(\frac{R_f}{\rho_0 f} \right) G_1 \left(\frac{\rho_0 f}{R_f} \right) \right] \quad (99)$$

$$K(\omega) = \gamma P_0 \left(\gamma - \frac{\gamma - 1}{1 + (1/i8\pi N_{pr} (\rho f / R_f)^{-1} G_2 (\rho f / R_f))} \right)^{-1} \quad (100)$$

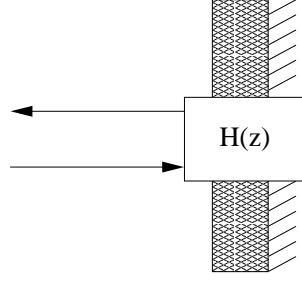


Figure 21: Modeling the surface with a transfer function $H(z)$.

where ρ is the density of air, N_{pr} is the Prandtl number, f is the frequency, R_f is the flow resistivity, γ is the specific heat ratio of air and P_0 is the air equilibrium pressure. The functions $G_1(\rho f/R_f)$ and $G_2(\rho f/R_f)$ are given by:

$$G_1(\rho f/R_f) = \sqrt{1 + i\pi(\rho f/R_f)}, \quad (101)$$

$$G_2(\rho f/R_f) = G_1[(\rho f/R_f)4N_{pr}], \quad (102)$$

For normal temperature and atmospheric pressure $\rho_0 = 1.2 \text{ kg/m}^3$, $N_{pr} = 0.702$, $\gamma = 1.4$ and $P_0 = 101320 \text{ N/m}^2$. Now the equations (99) and (100) can be written as:

$$\rho(\omega) = 1.2 + \sqrt{-\frac{0.0364}{(\rho_0 f/R_f)^2} - i\frac{0.1144}{\rho_0 f/R_f}} \quad (103)$$

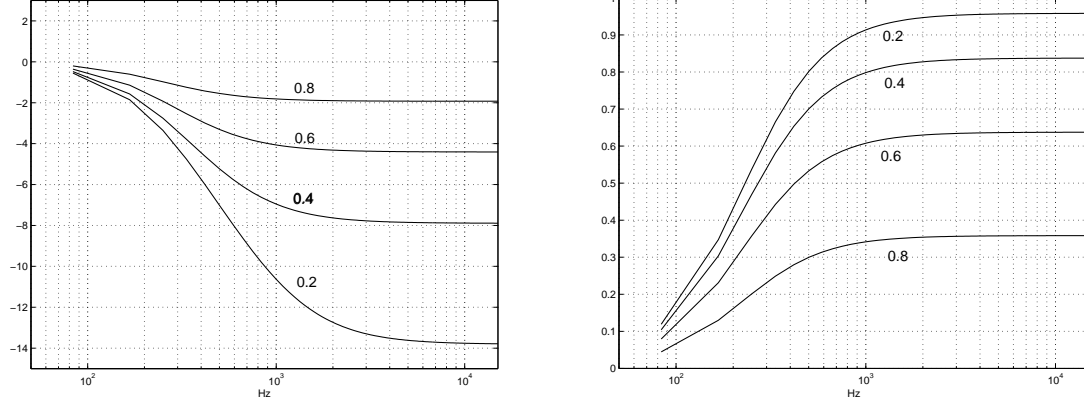
$$K(\omega) = 101320 \frac{i29.64 + \sqrt{\frac{2.82}{(\rho_0 f/R_f)^2} + i\frac{24.9}{\rho_0 f/R_f}}}{i21.17 + \sqrt{\frac{2.82}{(\rho_0 f/R_f)^2} + i\frac{24.9}{\rho_0 f/R_f}}} \quad (104)$$

5.3 Abstract models

If the general behavior of the material is known, any model that behaves the same way can be used as a system model for the surface. As in Figure 21, the surface under study can be considered to have a certain transfer function with a set of free parameters.

As an example, a low-order model is generated for a homogeneous wool-like absorbent on a hard wall. Considering the reflection from the surface such a system behaves very much like a low-pass filter. Thus, the system could be modeled by a first-order zero-pole filter $H_r(z)$

$$H_r(z) = \frac{k}{1 + az^{-1}} + b, \quad (105)$$



(a) Reflection coefficient

(b) Absorption coefficient

Figure 22: Different responses of the abstract model when $a = 0.99$ and b varies.

where b sets the high frequency gain. Equation (105) can also be written as

$$H_r(z) = \frac{k + b + abz^{-1}}{1 + az^{-1}}. \quad (106)$$

If the reflection at 0 Hz is assumed to be lossless the parameter k can be solved. Zero frequency corresponds to $z = 1$ in z-domain.

$$H_r(1) = 1 \Rightarrow \frac{k + b + ab}{1 + a} = 1 \quad (107)$$

$$k = 1 + a - b - ab \quad (108)$$

By substituting k into the original equation, a filter with two parameters is obtained.

$$H_r(z) = \frac{1 + a - ab + abz^{-1}}{1 + az^{-1}}. \quad (109)$$

The parameter b defines the gain (reflection coefficient) at high frequencies and the parameter a sets the “cutoff” frequency. Both of these parameters can be used as free parameters in curvefitting. Figures 22 and 23 illustrate the behavior of the model.

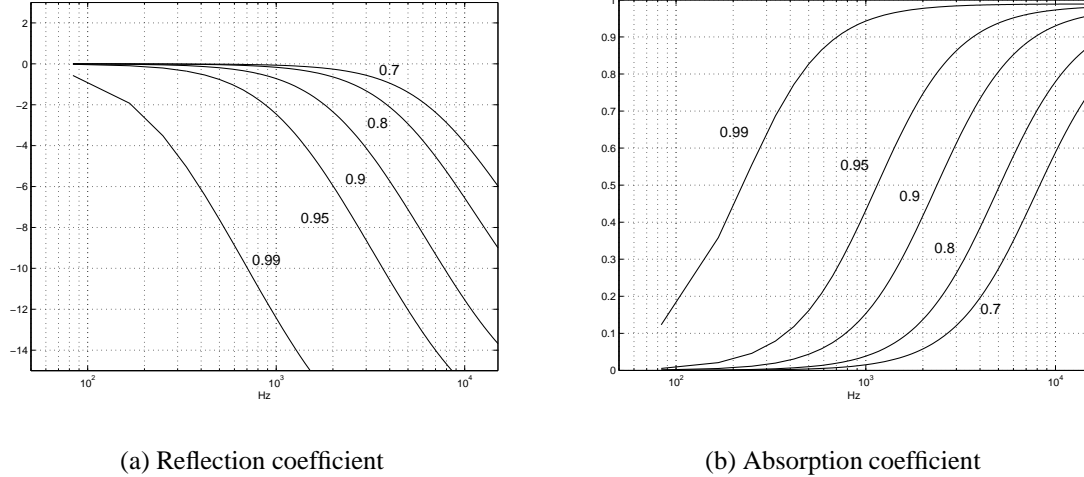


Figure 23: Different responses of the abstract model when $b = 0.1$ and a varies.

5.4 Curve fitting

Surface impedance measurement data can be used to calculate absorption and reflection coefficients and naturally the surface impedance as well. Curvefitting could be done to any of these quantities but in this case the fitting will be done to the reflection coefficient.

Depending on the used measurement technique the frequency range where the measurement data is accurate varies. The fitting should be done in the frequency range where the measurement data is accurate. Quite often the used time window sets the lower frequency limit and the measurement technique or the used model sets the higher frequency limit.

The fitting could be done by using any sophisticated curve-fitting algorithm. Since the optimization in most cases is nonlinear in the parameters used, a nonlinear curve-fitting technique must be used. In this work the MATLAB's function `lsqcurvefit()` is used. The `lsqcurvefit()` is a least-square based function that tries to find iteratively a value for a vector x that minimizes

$$\frac{1}{2}(F(x, xdata) - ydata)^2, \quad (110)$$

where $F(x, xdata)$ is the model function, x is the model's parameter vector, $xdata$ is the model's output and $ydata$ is measurement data.

As a result of the curve fitting a value for the model parameter vector x is obtained. With this parameter vector the model $xdata$ models the reflection at the surface of the material under study. The absorption coefficient can be easily calculated from this

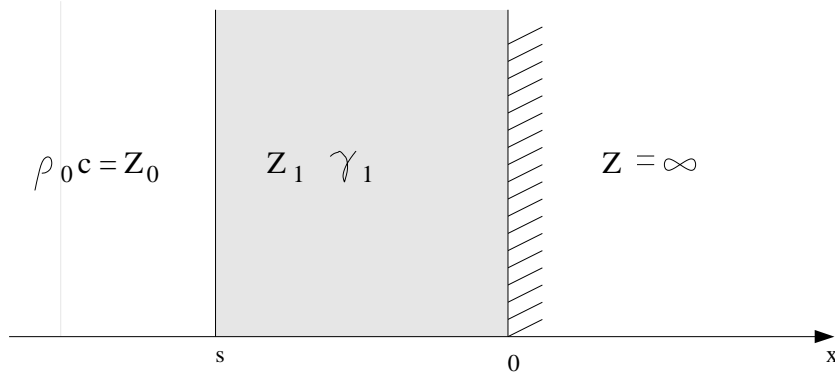


Figure 24: Material on a hard surface

data.

5.4.1 Fitting the propagation models

According to Equation (42) the characteristic impedance can be calculated anywhere in the material if the bounding impedances and the propagation constants are known. In a case where absorbent is placed on a hard surface (e.g. concrete wall) the impedance of the wall could be assumed to be infinite (See Figure 24). By substituting $Z = \infty$ to Equation (42) simplifies the equation for impedance in the material to

$$Z(x) = Z_1 \coth(\gamma_1 x). \quad (111)$$

The required quantities, the characteristic impedance Z_1 and the propagation constant γ_1 are hard to measure in-situ. The thickness of the material x is often known a priori. For fibrous-like absorbents the characteristic impedance and the propagation constant can be estimated with the empirical and the semi-empirical models presented in the previous chapters. All the physical models presented in this work are functions of flow resistivity R_f . By substituting these values to equation (111) the impedance becomes a function of flow resistivity

$$Z(x, R_f) = Z(R_f) \coth(\gamma(R_f)x). \quad (112)$$

If the thickness x is known the impedance at the surface becomes

$$Z(R_f) = Z(R_f) \coth(\gamma(R_f)s), \quad (113)$$

where s is the thickness of the material. Now, according to Equation (31) the reflection coefficient at the surface of the material can be written as

$$R(R_f) = \frac{Z(R_f) - \rho c}{Z(R_f) + \rho c} = \frac{z(R_f) - 1}{z(R_f) + 1}, \quad (114)$$

where $z(R_f) = Z(R_f)/(\rho c)$.

Equation (114) can be fitted to the measured reflection coefficient. As a result of the fitting, a value for the flow resistivity R_f is obtained. With this value Equation (114) is a complete model of the surface of the material.

5.4.2 Fitting the abstract system models

The abstract system model presented by Equation (109) is already a complete model of reflection at the surface of a homogeneous wool-like absorbent.

$$H_r(z) = \frac{1 + a - ab + abz^{-1}}{1 + az^{-1}}. \quad (115)$$

By using the parameters a and b as free parameters, the model can be fitted to a measurement data. As a result of the fitting, values for a and b are obtained. Now with these parameters Equation (109) is a complete model of a reflection at the surface of the material.

6 Results

In this thesis two new ideas were introduced to in-situ measurements: hard surface measurement as a reference for subtraction method (Chapter 3.4.1) and a model-based curvefitting for in-situ impedance measurement (Chapter 5). The measurements for both cases were done by using the subtraction method. For model-based curvefitting, any other method could have been used as well. Figure 25 shows the used measurement probe. The technical data of the specific hard- and software used is listed in Appendix A.2.4

The measurements were performed in a medium-sized foyer of a lecture hall. The free space between the walls was about six meters and the height of the foyer about five meters. The size of the measured material was 120 cm x 120 cm. The materials were placed and measured on the floor.

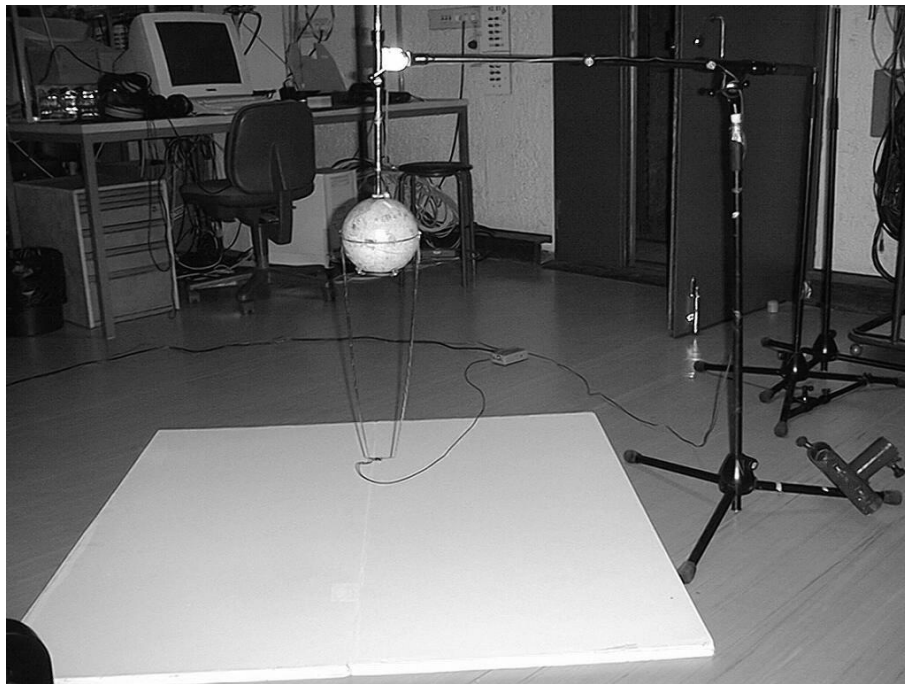


Figure 25: The measurement probe on a stand.

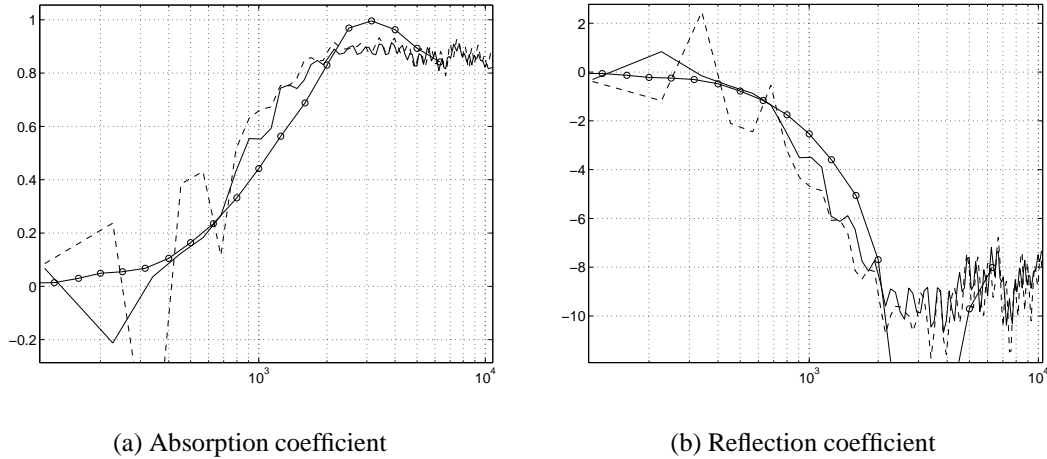


Figure 26: Absorption and reflection coefficients measured by using the subtraction technique. Dashed line is without and solid line is with the hard surface reference. The circled line is an impedance tube measurement of the same material (18 mm rock wool, density 40 kg/m^3).

6.1 Hard surface reference for subtraction method

Using the hard surface measurement as reference was tested on various materials. Figure 26 shows the results in a case where a rock wool specimen is placed on a hard floor. The bare floor was used as a hard surface for the hard surface measurement.

The fluctuation at low frequencies is effectively decreased compared to a case where a free-field measurement is used as reference although some non-physical values ($\alpha < 0$) still exist in the measurement data. More results can be found in Appendix B.1.2.

The hard-surface measurement should be performed in a way where the parasitic reflections are located in the same place in time as in the material measurements, but, e.g., with a wool-like absorbent on a hard surface some of the reflection occurs at the surface of the material and some at the hard surface behind the material. Both of these reflections will also occur as secondary reflections and these are impossible to cancel efficiently out with a hard surface reference.

6.2 Model-based curve fitting

The measurements for model-based curvefitting were performed by using the subtraction method. The models are fitted to the raw measurement data and the hard-surface referencing technique was not used. This way it can be seen how the model-based curvefitting works with corrupted measurement data.

In Figure 27 a 18 mm thick rock wool panel is measured on a hard floor and a model by Delany and Bazley is fitted to the measurement data. Figure 28 shows the same case with a model by Mechel fitted to the measurement data. With both models, the obtained results follow fairly well the impedance tube data. The Delany model seems to overestimate the absorption at low frequencies whereas the Mechel model gives non-physical, negative values. But in overall the method seems to give fairly good results.

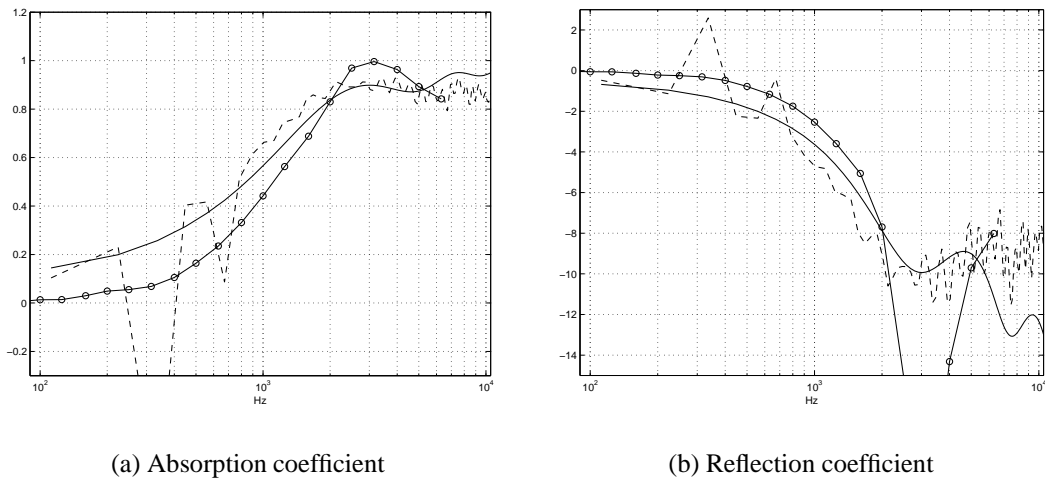
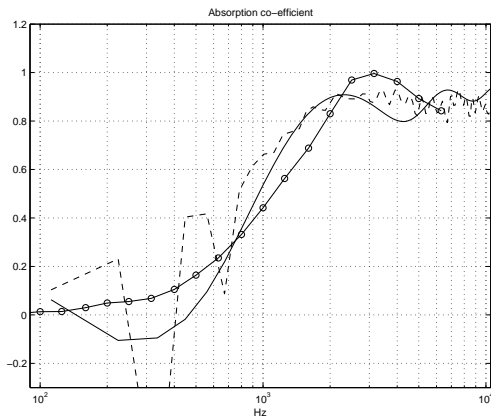
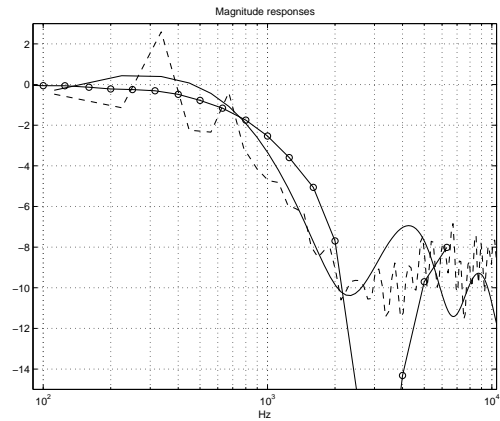


Figure 27: Delany-Bazley model fitted to the in-situ measurement data. Dashed line is the measurement data, solid line is the fitted model and the circled line is an impedance tube measurement of the same material (18 mm rock wool, density 40 kg/m^3).

Figure 29 shows an abstract model, introduced in chapter 5.3, fitted to the same measurement data. In this case, the model seems fit fairly well to the measured data. In general, and taking into account it's simplicity, this model worked quite well to measured data, especially at higher frequencies. More results can be found in Appendix B.1.2.

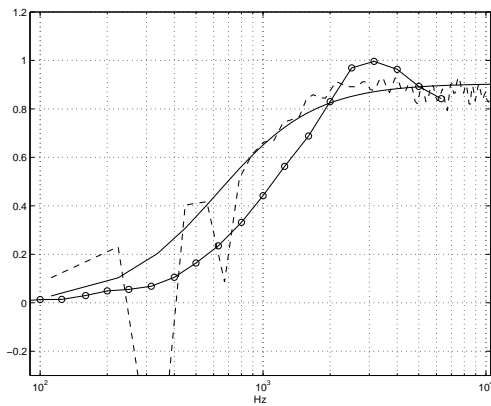


(a) Absorption coefficient

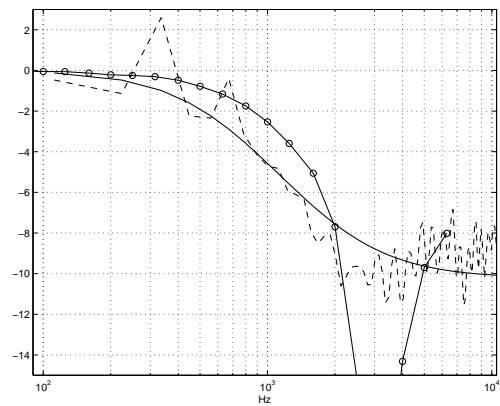


(b) Reflection coefficient

Figure 28: A model by Mechel fitted to the in-situ measurement data. Dashed line is the measurement data, solid line is the fitted model and the circled line is an impedance tube measurement of the same material (18 mm rock wool, density 40 kg/m^3).



(a) Absorption coefficient



(b) Reflection coefficient

Figure 29: An abstract model fitted to the measurement data. The dashed line is the in-situ measurement, solid line is fitted model and the circled line is an impedance tube measurement of the same material (18 mm rock wool, density 40 kg/m^3).

7 Discussion

A reliable in-situ measurement method would be a highly welcome tool for any acoustics designer. This work has studied various methods proposed in the past and even introduced some new ideas to improve the reliability of in-situ measurements. Still there is no method that would give good and reliable results covering the whole frequency band. Especially at low frequencies the quest for accuracy seems impossible to overcome. The theoretical and physical limits are hard to beat.

The model based curvefitting seems to be one interesting and promising way to add accuracy or at least reliability at low frequencies. The only and a hard requirement is the need for good and practical models. For simple cases this might not be a problem but in real measurement situations the surface structures are seldom simple.

When one is developing a measurement method the accuracy is always defined as how well the results with a new method compare to the so called reference methods. But what is the method that gives physically right results? The impedance tube method is the de facto reference method but in real spaces waves are not plane and reflections occur at all angles. The reverberation room method certainly is closer to a real life situation but such measurement are very tedious and the theory behind the calculations is fairly empirical. The data, obtained by the methods introduced in this work, fell mainly between the reverberation room and the impedance tube measurement data. But then again in many cases there were some non-physical values, such as negative absorption.

Of course, every method gives results according to the theory behind it. So, the applicability of any method relies on the knowledge and skills of the person performing the measurement or reading the measurement data. This applies to the reference methods as well as to in-situ methods. If the restrictions behind the measurement method are known and acknowledged, the in-situ methods can be used as tools for measuring the acoustical properties of materials.

8 Conclusions

In general, in-situ measurement techniques work fairly well in simple cases. Especially at the frequency range from few hundred Hz to few kHz and when measuring fairly absorptive materials the in-situ measurement techniques can give reasonably accurate results.

At lower frequencies and when measuring materials with little absorption, all the methods seem to fail. Using hard surface measurement as reference in the subtraction method seems to be one way to increase the reliability of the measurement at lower frequencies. But, even though the method gives “smoother” results, it should be used with great care until it has been studied more thoroughly.

The model-based curvefitting offers one way to improve the robustness of measurements, especially at low frequencies. The downside of the method is the need of practical models for materials and surface structures.

At the moment, the in-situ measurement methods do not compete in accuracy with traditional laboratory measurement techniques. But then again, when used by a skillful user the in-situ measurement techniques provide a useful and practical tool for an acoustics designer.

A Appendix

A.1 Materials

The materials measured in this work were provided by the manufacturers. In the measurements the material was placed on a concrete floor and sample sizes were 120 x 120 cm.

Aislo woodfibre damp slab

- thickness 50 mm
- density 75 kg/m³,



Isover Melody glass wool

- thickness 20 mm
- density 40 kg/m³
- (Figure illustrates a 50 mm version)



Paroc Fjord rock wool

- thickness 20 mm
- density 40 kg/m³



A.2 System setup

The system used for measurements consists of the following components:

- Microphone, Sennheiser KE 4-211
- 5.25" loudspeaker in a spherical enclosure
- Apple Macintosh computer
- QuickSig measurement software
- Adcom stereo amplifier
- UDMA10e Microphone preamplifier

Figure 30 shows a schematical drawing of the setup.

A.2.1 Microphone

The Sennheiser KE 4-211 electret microphone has a good response over a wide frequency range. The microphone is very omni-directional at the frequency range used in the measurements (50-10000 Hz).

A.2.2 Loudspeaker

The used loudspeaker was a closed box type with a 5.25 inch driver in a 1.8 liter enclosure (see Figure 25). The shape of the enclosure was chosen to be spherical to minimize the edge diffractions. The frequency response of the loudspeaker covers the needed frequencies for the measurements. This is essential for keeping the signal-to-noise ratio high enough. There are no strict requirements for the flatness of the response because of the measurement technique used.

A.2.3 Software

The QuickSig measurement software runs on a Apple Macintosh computer. The software is developed in the Laboratory of Acoustics and Audio Signal Processing at the Helsinki University of Technology [13]. The software is used to create the excitation signals and to record the data from the microphone. Impulse response is obtained by deconvolution computation The further processing is done with the MATLAB software.

A.2.4 Amplifiers

The Adcom stereo amplifier is used to drive the the loudspeaker. The amplifier is practically transparent in the measurement as long as the noise level is not too high, which is the case for this amplifier. If there were any deviations in the frequency response, the measurement technique would compensate it anyway.

The UDMPA10e Dual channel microphone preamplifier is used to boost the microphone signal up to line level. The amplifier has a flat frequency response from 20 - 200000 Hz (+0.0/0.5 db). At the maximum gain the S/N ratio is 71 dB and the THD at 1 kHz is 0.4 %. [32]

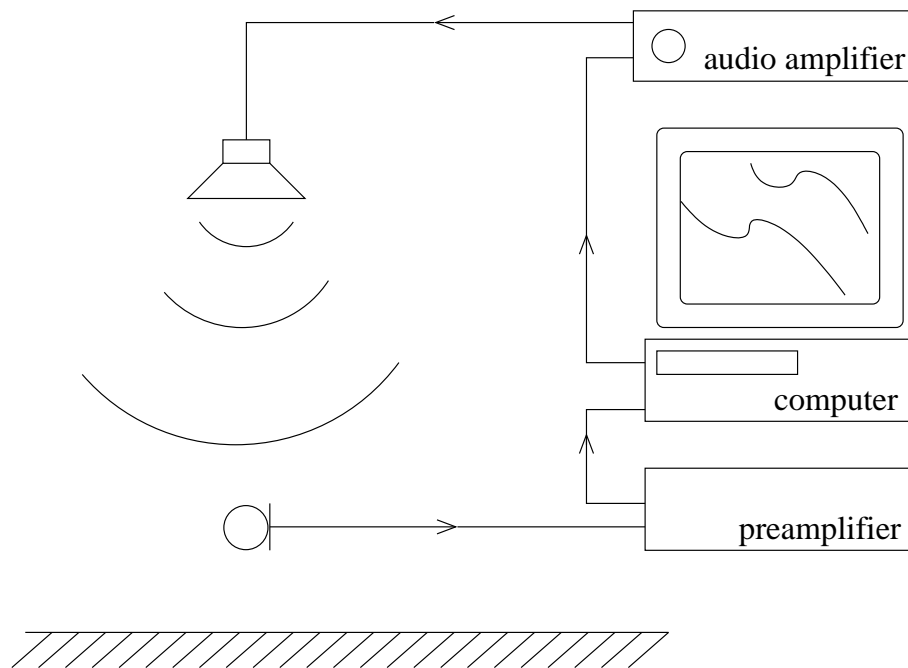


Figure 30: Schematic diagram of the measurement system.

B Appendix

B.1 Measurement data

B.1.1 Using hard surface as reference

In the following the measurements are performed by using the subtraction method proposed by Mommertz and by using hard surface measurement as reference. The results are compared with impedance tube measurements.

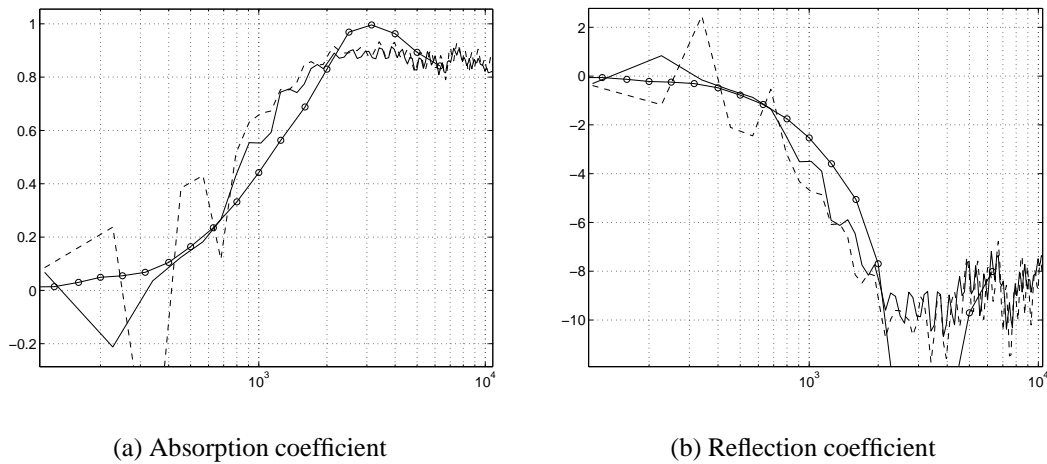
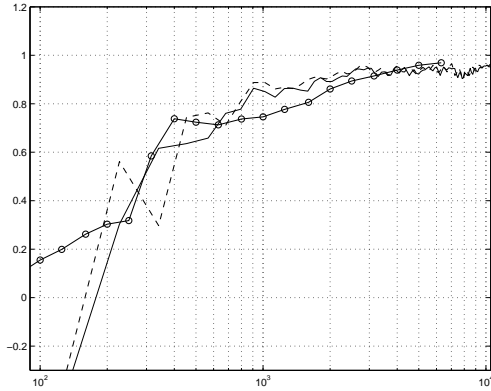
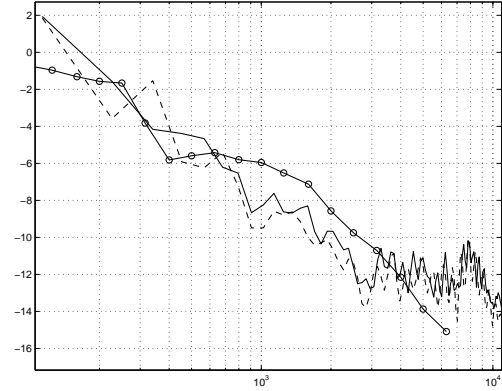


Figure 31: Absorption and reflection coefficients measured by using the subtraction technique. - - - in-situ measurement, — hard surface reference, -o-o- impedance tube. (18 mm rock wool, density 40 kg/m³)

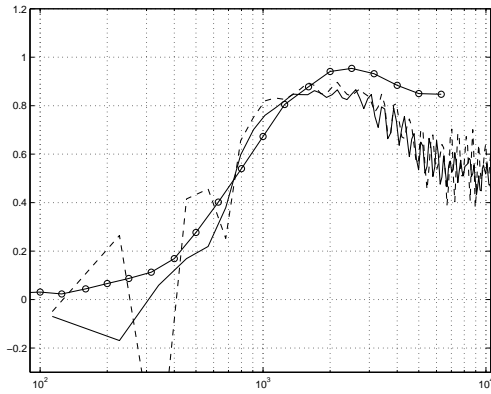


(a) Absorption coefficient

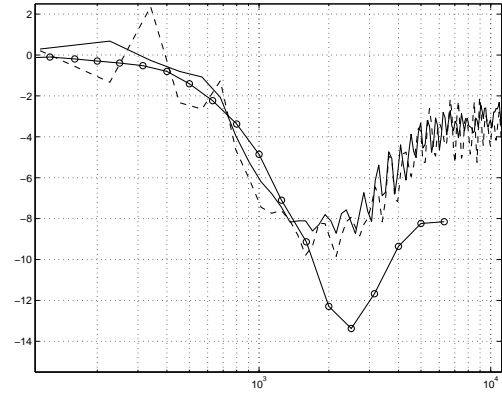


(b) Reflection coefficient

Figure 32: Absorption and reflection coefficients measured by using the subtraction technique. - - - in-situ measurement, — hard surface reference, -o-o- impedance tube. (50 mm wood fiber, density 75 kg/m³)



(a) Absorption coefficient



(b) Reflection coefficient

Figure 33: Absorption and reflection coefficients measured by using the subtraction technique. - - - in-situ measurement, — hard surface reference, -o-o- impedance tube. (20 mm glass wool, density 40 kg/m³)

B.1.2 Model-based curvefitting

In the following the model-based curvefitting is applied to in-situ measurement data. The measurements are performed by using the subtraction method. Hard surface measurement has not been as reference here. The propagation models by Delany and Bazley and by Mechel are tested. Also an abstract model introduced in Chapter 5.3 is tested. The results are compared with impedance tube measurements.

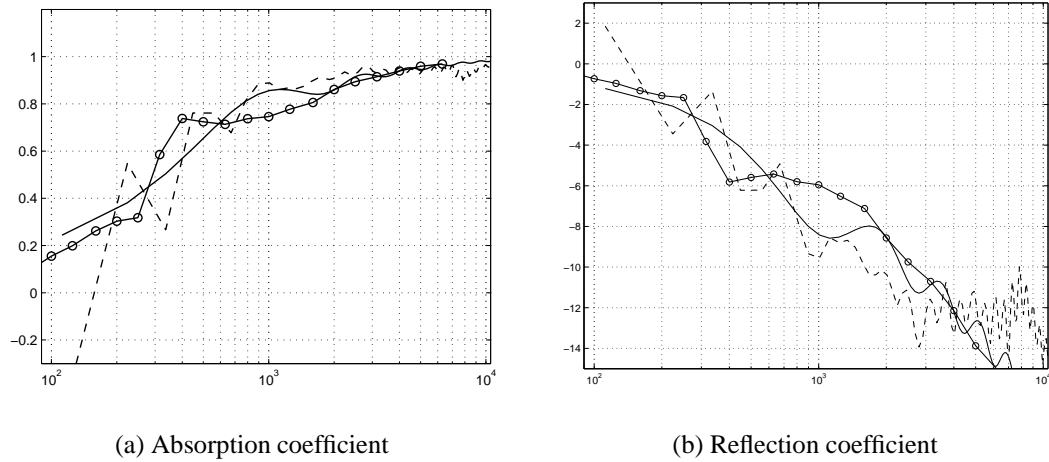
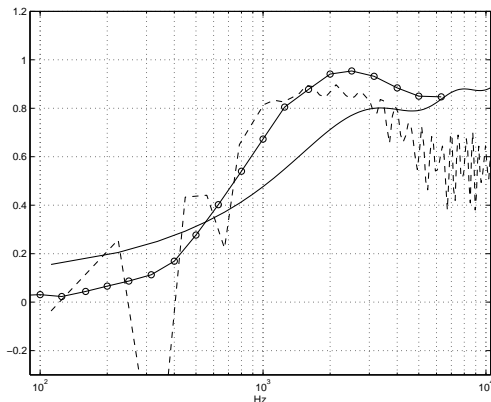
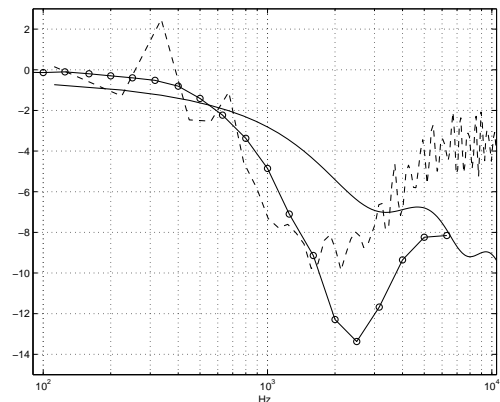


Figure 34: A Delany-Bazley model fitted to measurement data. - - - in-situ measurement, — fitted model, -o-o- impedance tube. (50 mm wood fiber, 70 kg/m³)

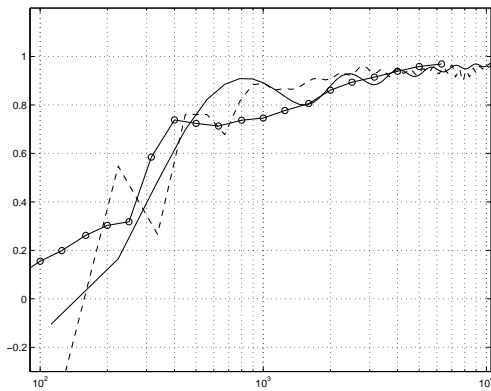


(a) Absorption coefficient

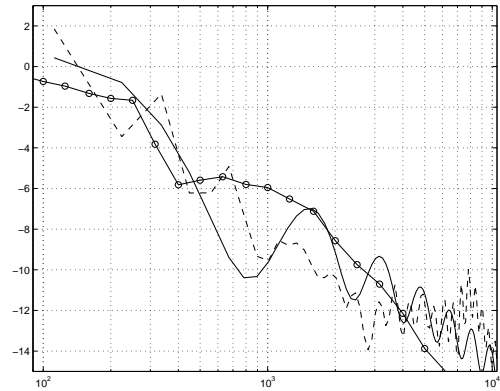


(b) Reflection coefficient

Figure 35: A Delany-Bazley model fitted to measurement data. - - - in-situ measurement, — fitted model, -o-o- impedance tube. (20 mm glass wool, 40 kg/m³)

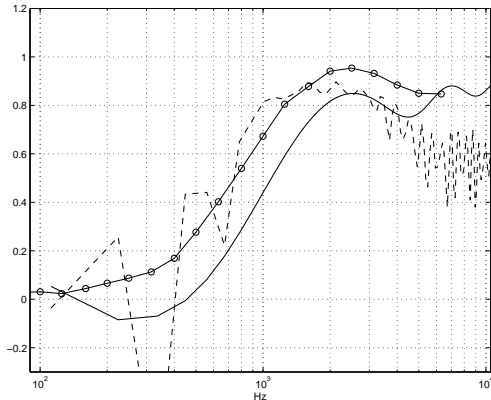


(a) Absorption coefficient

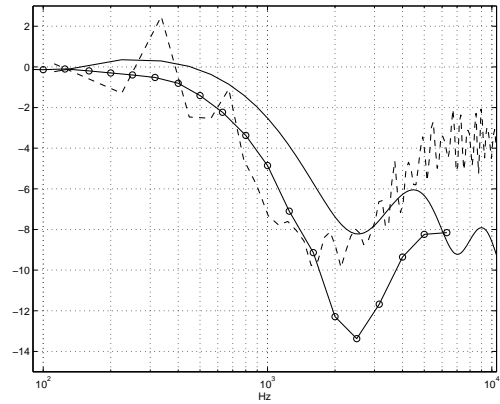


(b) Reflection coefficient

Figure 36: A model by Mechel fitted to in-situ measurement data. - - - in-situ measurement, — fitted model, -o-o- impedance tube. (50 mm wood fiber, density 75 kg/m³)

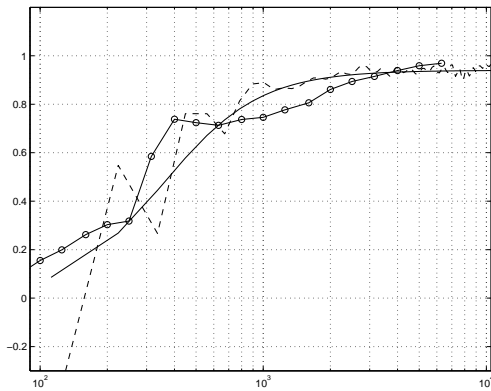


(a) Absorption coefficient

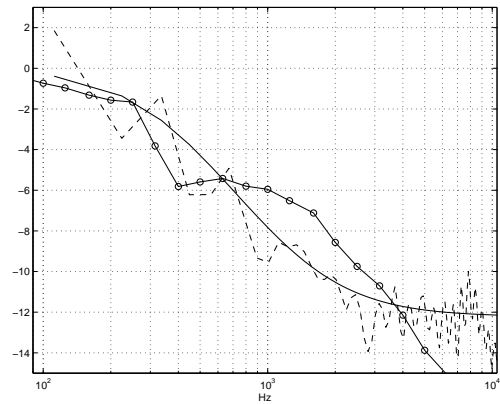


(b) Reflection coefficient

Figure 37: A model by Mechel fitted to in-situ measurement data. - - - in-situ measurement, — fitted model, -o-o- impedance tube. (20 mm glass wool, density 40 kg/m³)

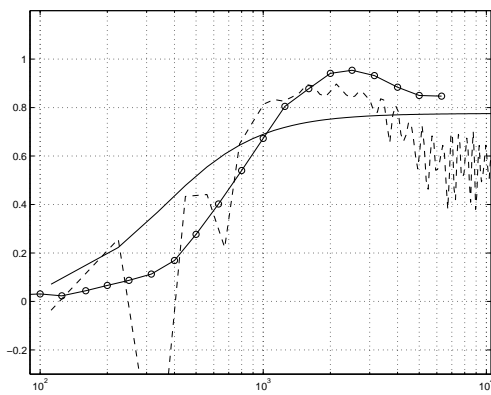


(a) Absorption coefficient

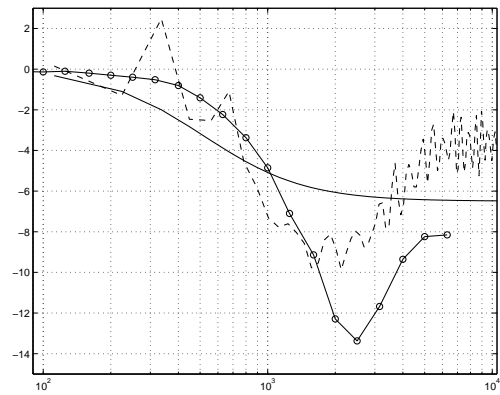


(b) Reflection coefficient

Figure 38: An abstract model fitted to in-situ measurement data. - - - in-situ measurement, — fitted model, -o-o- impedance tube. (50 mm wood fiber, density 75 kg/m³)



(a) Absorption coefficient



(b) Reflection coefficient

Figure 39: An abstract model fitted to in-situ measurement data. - - - in-situ measurement, — fitted model, -o-o- impedance tube. (20 mm glass wool, density 75 kg/m³)

References

- [1] Allard J.F and Sieben B., “Measurements of acoustic impedance in a free field with two microphones and a spectrum analyzer”, *The Journal of Acoustical Society of America*, vol. 77(4), pp. 1617-1618, 1984.
- [2] Allard J.F. and Champoux Y., “In situ two-microphone technique for the measurement of the acoustic surface impedance of materials”, *Noise Control Engineering Journal*, vol. 32/Number 1, pp. 15-23, Jan-Feb 1989.
- [3] Allard J.F. and Champoux Y., “New empirical equations for sound propagation in rigid frame fibrous materials”, *The Journal of Acoustical Society of America*, vol. 91(6), pp. 3346-3353, June 1992.
- [4] Alonso M. and Finn E.J., *Fundamental university physics, volume II, Fields and waves*, Addison-Wesley publishing company, 2nd Edition, 1983.
- [5] Champoux Y. and Richarz W.G., “An aid in the numerical integration for in situ acoustic impedance and absorption coefficient measurements”, *The Journal of Acoustical Society of America*, vol. 87(4), pp. 1809-1812, April 1990.
- [6] Chung J.Y. and Blaser D.A., “Transfer function of measuring in-duct acoustic properties”, *The Journal of Acoustical Society of America*, 68(3), pp. 907-913, 1980.
- [7] Delany M.E., Bazley E.N. “Acoustical properties of fibrous absorbent material”, *Applied Acoustics*, (3), pp. 105-116, 1970.
- [8] Dutilleul G., Vigran T.E. and Kristiansen U.R., “An in situ transfer function technique for the assessment of the acoustic absorption of materials in buildings”, *Applied Acoustics*, vol. 62, pp. 555-572, 2001.
- [9] Farina A., “Simultaneous Measurement of Impulse Response and Distortion with a Swept-Sine Technique”, Reprint 5093, AES 108th Convention, Feb. 2000, Paris, France.
- [10] Garai M., “Measurement of the Sound-Absorption Coefficient In-Situ: The Reflection Method Using Periodic Pseudo-random Sequences of Maximum Length” *Applied Acoustics*, vol. 39, pp. 119-139, 1993.
- [11] Green E.R., “Measurement System for Acoustic Absorption Using the Cepstrum Technique” in *Proceedings of the 2002 International Congress and Exposition on Noise Control Engineering (Inter-noise 2002)*, August 19-21, 2002.

- [12] Ingård U. and Bolt R.H., “A free field method of measuring the absorption coefficient of acoustic materials”, *The Journal of Acoustical Society of America*, vol. 23(5), pp. 509-516, 1951.
- [13] Karjalainen, M., “Object-Oriented Programming: A Case Study of QuickSig”, *IEEE Acoustics, Speech and Signal Processing Magazine*, pp. 21-31, 1990.
- [14] Karjalainen M. and Tikander M., “Reducing Artifacts of In-situ Surface Impedance Measurement”, in *Proceedings of the 17th Int. Congr. on Acoust. (ICA)*, vol. 2, p. 393, Rome, Italy, September 2-7., 2001.
- [15] Klein C. and Cops A., “Angle dependence of the impedance of a porous layer”, *Acta Acustica*, vol. 44, pp. 258-264, Jan-Feb 1980.
- [16] Kuttruff H, *Room Acoustics*, Elsevier Science Publisher Ltd, 4th ed., 1999.
- [17] Lahti T., *Akustinen mittaustekniikka*, Helsinki Univ. of Tech., Laboratory of Acoustics and Audio Signal Processing, Report Series 38, Otaniemi 1995.
- [18] Mechel F.P., Beranek L (ed.) *Noise and Vibration Control Engineering*, John Wiley & Sons, New York 1992,
- [19] Mommertz E. and Müller S., “Measuring Impulse Responses with Digitally Pre-emphasized Pseudorandom Noise Derived from Maximum-Length Sequences”, *Applied Acoustics*, 44, pp. 195-214, 1995
- [20] Mommertz E., “Angle dependent in situ measurement of the complex reflection coefficient using a subtraction technique”, *Applied Acoustics*, vol. 46, 1995, pp. 251-263.
- [21] Morse P.M., *Vibration and sound*, McGraw-Hill Book Company, Inc., Second edition, 1948.
- [22] Morse P.M. and Ingard K.U., *Theoretical Acoustics*, McGraw-Hill Book Company, Inc., 1968.
- [23] Nobile M.A. and Hayek S.I., “Acoustic propagation over an impedance plane”, *The Journal of Acoustical Society of America*, vol. 78(4), pp. 1325-1336, October, 1985.
- [24] Nocke C. et al., “Impedance deduction from broad-band, point-source measurements at grazing incidence”, *Acta Acustica*, Vol 83, pp. 1085-1090, 1997.
- [25] Nocke C., “In-situ acoustic impedance measurement using a free-field transfer function method”, *Applied Acoustics*, Vol 59, pp. 253-264, 2000.

- [26] Nocke C., “Improved Impedance Deduction from Measurement near grazing incidence”, *Acta Acoustica* vol. 85, pp. 589-590, 1999.
- [27] Rossing T.D., *The Science of Sound*, Addison-Wesley Publishing Company, Inc., 2nd ed., 1990.
- [28] Rudnick I., “The propagation of an acoustic wave along a boundary”, *The Journal of Acoustical Society of America*, vol. 19(2), pp. 348-356, 1947.
- [29] Stan G-B., Embrechts J-J and Archambeau D, “Comparison of Different Impulse Response Measurement Techniques”, *The Journal of Acoustical Society of America*, vol.50(4), pp. 249-262, 2002.
- [30] Tikander M. and Karjalainen M., “Model Based Curve Fitting for In-situ Surface Impedance Measurement”, in *Proceedings of the Joint Baltic-Nordic Acoust. Meeting 2002*, August, 2002.
- [31] Toivanen J., *Teknillinen Akustiikka*, Otakustantamo, Espoo, 1978.
- [32] Unides Design Avoin Yhtiö, MPA10e Dual Channel Microphone Preamplifier data sheet, Helsinki, Finland, 2001.